

Effect of Area-Filling Path on the Residual Stresses Developed During Weld-Deposition Based Additive Manufacturing

Robin Mathews

A Dissertation Submitted to
Indian Institute of Technology Hyderabad
In Partial Fulfillment of the Requirements for
The Degree of Master of Technology



भारतीय प्रौद्योगिकी संस्थान हैदराबाद
Indian Institute of Technology Hyderabad

Department of Mechanical Engineering

July, 2013

Declaration

I declare that this written submission represents my ideas in my own words, and where others' ideas or words have been included, I have adequately cited and referenced the original sources. I also declare that I have adhered to all principles of academic honesty and integrity and have not misrepresented or fabricated or falsified any idea/data/fact/source in my submission. I understand that any violation of the above will be a cause for disciplinary action by the Institute and can also evoke penal action from the sources that have thus not been properly cited, or from whom proper permission has not been taken when needed.

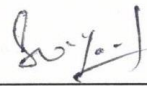
A handwritten signature in black ink, appearing to read 'Robin Mathews', written in a cursive style.

Robin Mathews


ME11M15

Approval Sheet

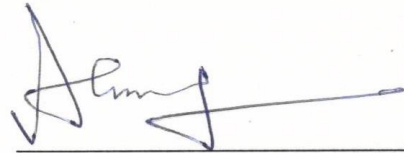
This thesis entitled “Effect of Area-Filling Path on the Residual Stresses Developed during Weld-Deposition Based Additive Manufacturing” is approved for the degree of Master of Technology from IIT Hyderabad.



Dr. S. Suryakumar, IIT Hyderabad
Adviser



Dr. Venkata Reddy N, IIT Hyderabad
Internal Examiner



Dr. A. Venugopal Rao, DMRL
External Examiner



Dr. Bharat Bhooshan Panigrahi, IIT Hyderabad
Chairman

Dedicated to

My beloved family

Abstract

There is an increasing interest in the industry for using Additive Manufacturing techniques not just for prototyping but for actual applications too. For this to happen, various constraints in commercialization of the metallic components made by using additive manufacturing have to be overcome. Management of thermally induced residual stresses during the deposition of metal is one of the major challenges that need to be addressed. With the help of numerical and experimental methods, this paper studies effect of area filling paths on the residual stresses developed during weld-deposition. Finite element analysis is done using ANSYS Mechanical APDL for different area filling paths. The temperature gradient and the thermally induced residual stress produced during material deposition are predicted using finite element analysis. The obtained results were validated with the help of experiments. A GMAW welding system was attached to the CNC to create the desired area filling pattern. The residual stresses were measured using a XRD system. The process parameters used in the finite element study and experiments were based on initial trials carried out to determine the operatable range of parameters. Three area-filling patterns viz., zig-zag, contour (outside-in) and contour (inside-out) were analyzed; maximum residual stress concentration was found to occur in the case of contour (outside-in).

Nomenclature

q- Heat flux

E- Modulus of elasticity

C- Distribution coefficient

t- Time

ρ - Density of material

c- Specific heat capacity of material

k- Thermal conductivity

η - Arc efficiency

U- Voltage

I- current

S- Weld torch speed

h- Heat transfer coefficient

T- Temperature

ϵ_0 - Emissivity

σ_0 - Stefan–Boltzmann constant

Contents

Declaration	ii
Approval Sheet.	iii
Acknowledgement	iv
Abstract	vi
Nomenclature	vii
1. Introduction	1
1.1. Additive Manufacturing	1
1.1.1. Classification of additive manufacturing process	3
1.1.1.1. Laminated manufacturing	3
1.1.1.2. Powder bed technology	4
1.1.1.3. Deposition technology	6
1.2. Area filling	7
1.3. Problem definition	8
1.4. Objective of study	9
2. Literature Survey	10
2.1. Introduction	10
2.2. Modeling of weld deposition for residual stress	10
2.3. Studies on induced residual stress during metallic AM	12
2.4. Summary	13
3. Finite Element Analysis of the Deposition Pattern	14
3.1. Introduction	14
3.2. Governing Equation and Finite Element Evaluation	14
3.2.1. Gaussian heat distribution	14
3.2.2. Assumption of finite element analysis	16

3.3. Boundary Conditions	16
3.3.1. Thermal boundary conditions	17
3.3.2. Mechanical boundary Conditions	18
3.4. Process parameters used for analysis	18
3.5. Finite element implementation of the problem in ANSYS Mechanical APDL	19
3.5.1. Selection of the element type	19
3.5.2. Modeling of plate and weld Path	22
3.5.3. Material Properties	22
3.5.4. Application of Heat Flux	23
3.5.5. Iteration of the results for Subsequent elements	23
3.6. Simulation Results	25
3.6.1. Zigzag area filling pattern	25
3.6.2. Inside out contour area filling pattern	26
3.6.3. Outside in contour area filling pattern	27
3.7. Summary	28
4. Experimental Validation	29
4.1. Introduction	29
4.2. Initial trials for determining the operatable welding parameters	29
4.3. Experimental Setup	33
4.3.1. Fixture design	33
4.3.2. Weld deposition system	34
4.3.3. Residual stress measurement system.	36
4.4. Experimental procedure	38
4.5. Comparison of experimental and modeling results	40
4.6. Summary	44
5. Conclusion and Future Scope	45

5.1. Conclusion	45
5.2. Future Scope	46
Reference	47

List of Figures

1.1	Slicing in additive manufacturing	1
1.2	Additive manufacturing process	2
1.3	Classifications of additive manufacturing	3
1.4	Laminated object manufacturing	4
1.5	Powder bed technology (Selective Laser Sintering)	5
1.6	Deposition technology (LENS Process)	6
1.7	Different types of area filling methods	7
1.8	Different types of contour area filling methods. a) Outside-in contour filling b) Inside-out contour filling	8
2.1	Longitudinal change in residual stress along weld bead	11
2.1	Change in residual stress with respect to welding speed	12
3.1	Circular disc heat source	15
3.2	Boundary condition for thermal analysis	17
3.3	Boundary conditions for structural analysis	18
3.4	Selected area filling options for analysis	19
3.5	Flow chart of analysis plan in ANSYS APDL	20
3.6	Finite element model a) Finite element model of the base plate and weld path b) Zoomed view of the finite element model of weld path	21
3.7	Solid 5 element	22
3.8	Properties of EN08 as a function of temperature a) Thermal conductivity, b) Specific heat, c) Density d) Modulus of elasticity e) Coefficient of thermal expansion	24
3.9	Zigzag area filling path pattern along with the path a) Temperature distribution. b) Stress distribution	25
3.10	Inside-out contour area filling path pattern along with the path a) Temperature distribution. b) Stress distribution	26
3.11	Outside-in contour area filling path pattern along with the path a) Temperature distribution. b) Stress distribution	27

4.1	Weld beads obtained for different welding currents with weld speeds ranging from .5m/min to 3m/min	30
4.2	Deposition patterns obtained with step over increment 5mm a) With step over increment 5 mm contour path b) With an increment 5mm zigzag path	31
4.3	Deposition patterns obtained using stopover increment 3mm	32
4.4	Fixture design	34
4.5	Fixture to retain residual stress of the base plate a) side view of the assembled fixture a) Top view of the fixture c) Isometric view from the bottom d) Fixture and base plate disassembled	35
4.6	AGNI BVM 40 TC20 vertical machining center with Fanuc controller	36
4.7	EVM Taurus 551 synergic GMAW system	36
4.8	Retro fitment on CNC machine	37
4.9	Proto x ray residual stress measurement instrument	38
4.10	Different area filling patterns specimens a) Zigzag area filling pattern b) Outside-in contour area filling pattern c) Inside-out contour area filling pattern	39
4.11	Direction of measurement in XRD	40
4.12	Stress distribution on the outside-in contour area filling path a)Experimental result b) simulation result	41
4.13	Crack formed during outside -in contour	42
4.14	Stress distribution on the inside-out contour area filling path a)Experimental result b) simulation result	42
4.15	Stress distribution on the outside-in contour area filling path a)Experimental result b) simulation result	43

Chapter 1

Introduction

1.1 Additive manufacturing

Additive manufacturing (AM) is the process of manufacturing three-dimensional solid object from a CAD model. Models are generated as successive 2D layers in different shapes and finally realized as 3D solid, as shown in fig 1.1 [1]. Hence, complex self-assembled models, which are not possible using conventional subtractive processes, can be made. It also eliminated process planning, facilitating the direct manufacture of parts.

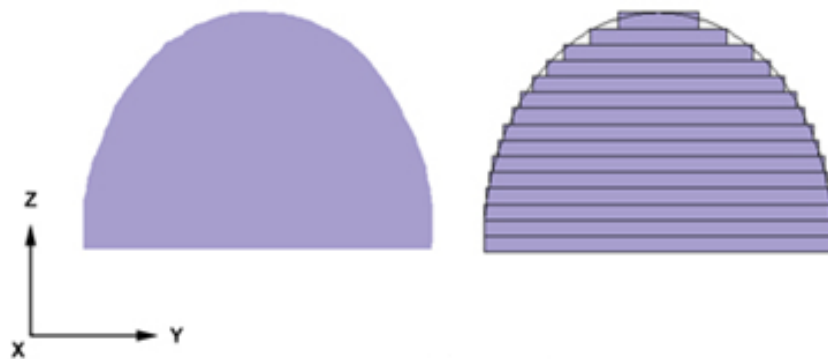


Figure 1.1 : Slicing in additive manufacturing [2]

In comparison to subtractive manufacturing (SM) techniques like machining, additive manufacturing processes have high production time and cost. However, the SM methods are incapable of producing complicated geometries like self-assembled parts and build in models. Additive Manufacturing technologies offer better advantages in terms of less product development time, shape complexity and ability to realize objects with gradient properties.

Initially, AM was used by industries to create the prototype of the final product before commercialization, so as to provide a rough idea about the product and to obtain feedback. But now it is used to create the parts meant for final use too. Thus, during its evolution, Additive Manufacturing was

referred using various terms like Rapid prototyping, Rapid Tooling, Rapid Manufacturing, Solid Freeform Fabrication, 3D Printing before arriving on the term additive manufacturing, thanks to the latest ASTM standards on its terminology [1].

There are a number of steps that are involved, ranging from creating a CAD file to realization of physical form as shown in fig 1.2. Simple products make use of AM only, while complex and higher engineering parts adopts numerous stages and iterations during the development stage.

Various processes that are involved in the additive manufacturing process are

- 1 Development of CAD file
- 2 Conversion to STL format
- 3 Transferring file to machine
- 4 Changing machine settings
- 5 Building model
- 6 Removal process and cleaning
- 7 Post-processing of the part
- 8 Applications

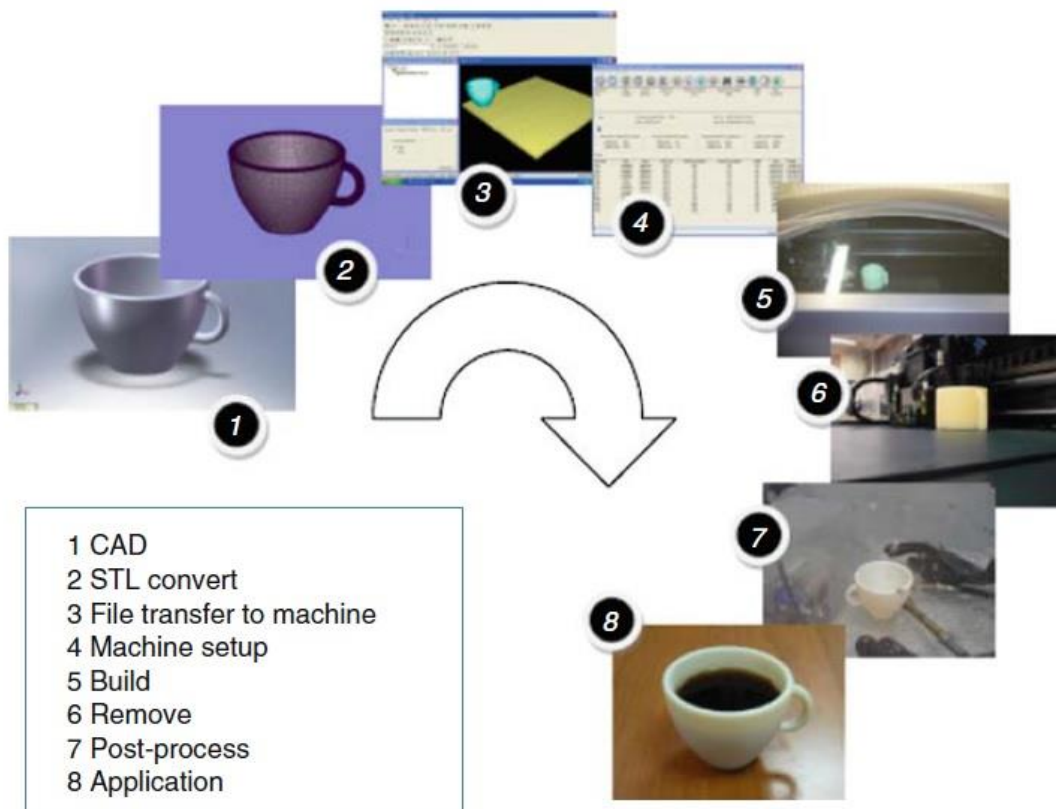


Figure 1.2: Additive manufacturing process [1]

1.1.1 Classification of Additive manufacturing Process

The additive manufacturing process can be classified into different types based on the technology and the type of raw materials used as shown in Fig 1.3

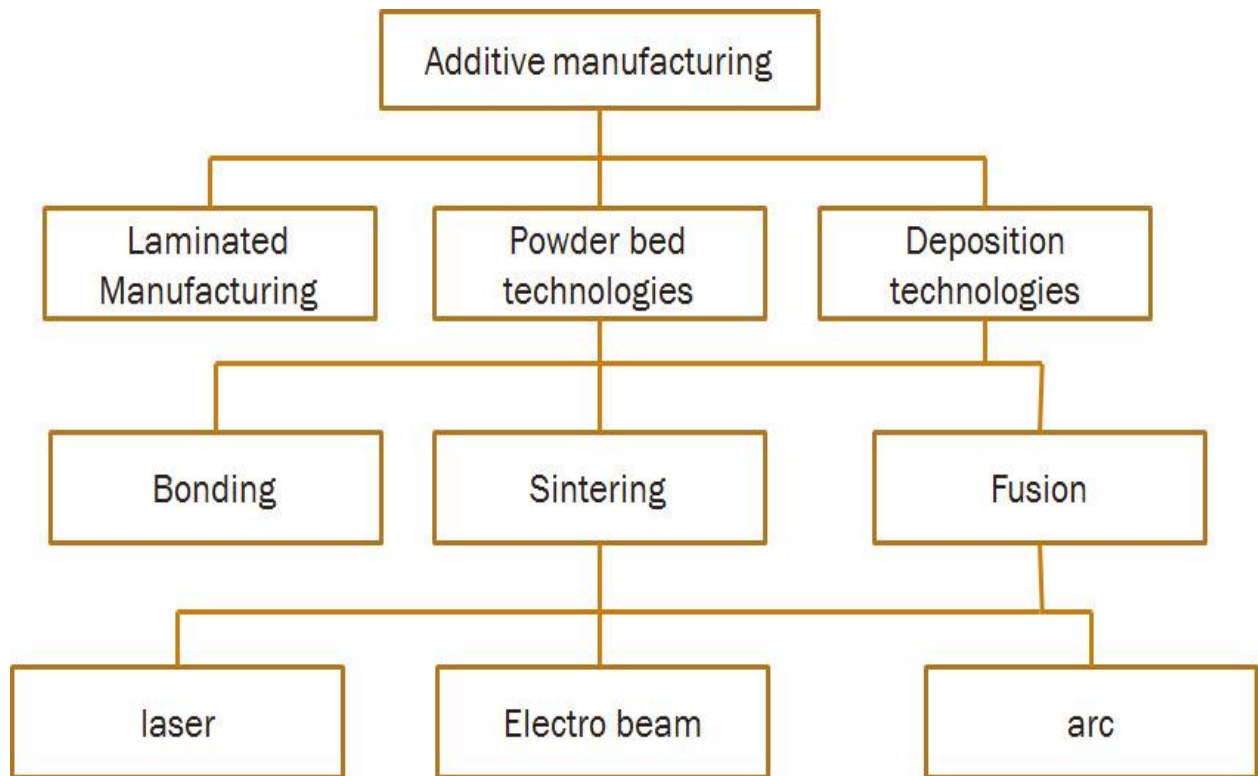


Figure 1.3: Classifications of additive manufacturing

1.1.1.1 Laminated manufacturing:

The first commercialized sheet laminated process is sheet laminated object manufacturing (LOM) and is developed by Helisys Inc. (Cubic Technologies is now the successor organization of Helisys)

In this process, paper is laminated in layer by layer fashion and cutting is done by laser or by sharpened blades. There are many laminated manufacturing techniques that build different materials and cutting techniques. This process is robust, flexible and valuable for many applications. And layered cross section can be manufactured quickly since trimming is required only in the boundary not like other AM process. Laminated object manufacturing can be classified into further forms like 1) gluing or adhesive bonding, 2) thermal bonding processes 3) clamping, and 4) ultrasonic welding.

In gluing or adhesive bonding process materials are cut into the required shape and are pasted one over the other using adhesive agents. The raw material for this process is mostly paper and it is shaped using either laser or cutting blades. The adhesive agents used for bonding are thermoplastic pastes.

Thermal bonding process is mainly for manufacturing metallic objects. Bonding is done by diffusion bonding, laser spot welding, and brazing techniques. This method is found to be effective in manufacturing complex metallic parts especially for the one with a cavity or with channels. The major difficulty in this process is the removal of support material.

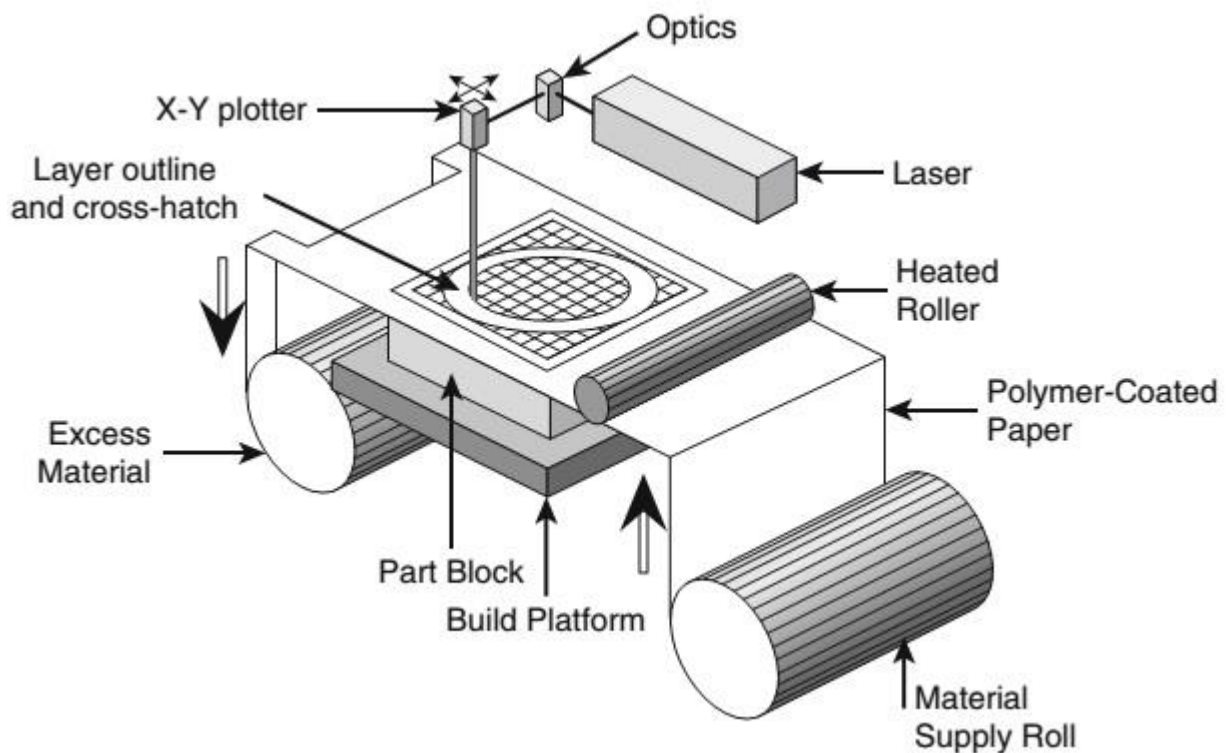


Figure 1.4: Laminated object manufacturing [3]

1.1.1.2 Powder bed technology

It is one among the first commercialized AM product. Selective laser Sintering (SLS) which was developed at the University of Texas at Austin, USA, was the first to be commercialized. In the powder bed fusion process a layer of raw material in powdered form is spread over the platform, then the desired shape is obtained by creating a solid shape. The separate support mechanism is not required since the unsolidified surface remains and acts as a support mechanism. Powder bed technology can be classified into four different mechanisms [4]: Solid state sintering, chemically induced binding, liquid-phase sintering and full melting.

In the solid state fusion process powdered particle diffuses with each other at high temperature without melting. As the temperature at which the diffusion occurs elevates porosity of the solid particle increases.

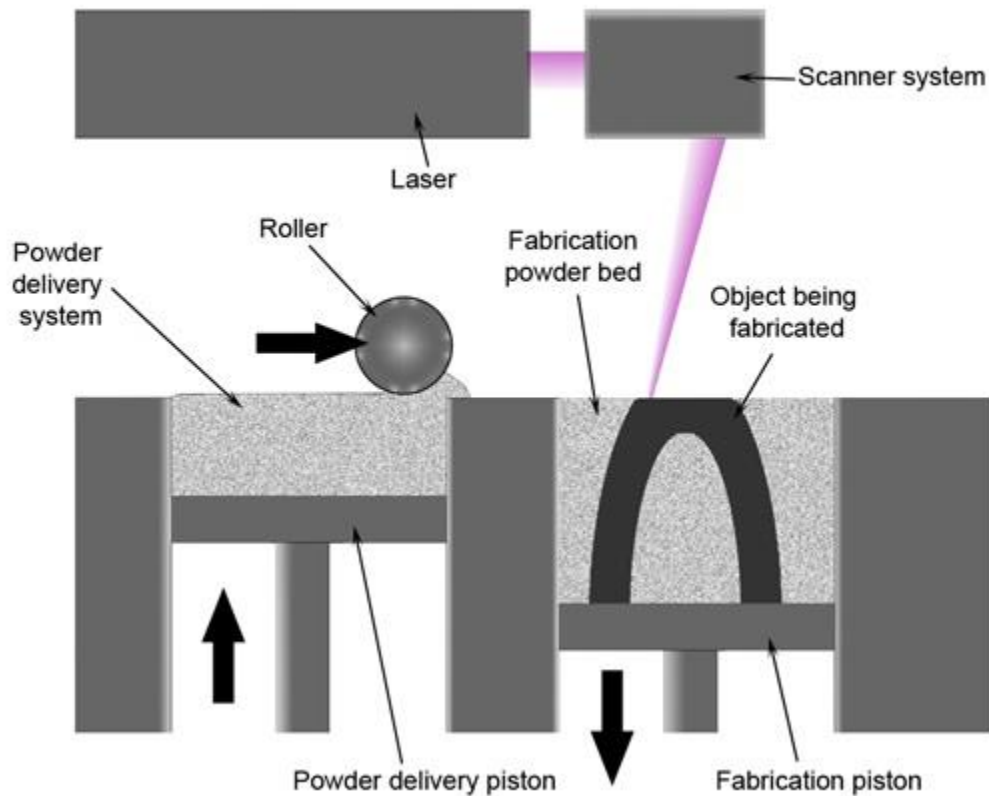


Figure 1.5: Powder bed technology (Selective Laser Sintering) [5]

In chemically induced sintering process, thermally active chemical reaction is induced in between powdered particle either by adding chemically reactive particles or by reaction between the powdered materials itself. Similar to solid state sintering process, porosity is the main issues in chemically induced sintering, so the parts produce need to undergo post processes like infiltration or high temperature furnace sintering. In bonding process, powdered particles adhere to each other by thermally active chemical reaction between powders of different types or between atmosphere gas and powder that results in the byproduct that adheres the powder together. In the sintering processes, external heat is used to melt the powdered particles partially so that the particles stick together to form a solid. Liquid phase sintering one of the most commonly used powder bed technology. In this process, the constituents added with the powdered material melts and bind the material together to form a solid model. As a reason higher temperature melting point materials can be bound together. The different ways in which liquid base sintering can be utilized which is explained by Kruth et al. [4]. Full melting process is used for metal alloys and semi crystalline polymers. In this method the entire material is melted and fused

with each other to form solid substance. Here the heat provided from the laser or a beam source is sufficient enough to melt the powder bed layer and previously solidified layer of material. In full melting process, due to rapid melting and cooling process, unexpected properties arise which may be favorable [6].

1.1.1.3 Deposition technologies

Deposition technology enables the creation of parts by deposition of molten or semi melted materials from powdered or wire feed stock .This method is mainly used for metals, but it can also be used for non-metals like plastics, ceramics, and composites [1]. In beam deposition (BD) technology narrow beam of energy is used to heat and melt the material that is about to be deposited. Unlike powder bed technology, in BD technology, material is melted as they are deposited, rather than melting a bed of powdered material. There are different type of BD methods based on various parameters such as source of laser power, laser spot size, laser type, powder delivery method, inert gas delivery method, feedback control scheme, and/or the type of motion control utilized , they are Laser Engineered Net Shaping (LENS), Direct Metal Deposition (DMD), Directed Light Fabrication (DLF), 3D Laser Cladding, Laser Generation, Laser-Based Metal Deposition (LBMD), Laser Direct Casting, Laser Freeform Fabrication (LFF), Laser Cast, Laser Consolidation, LasForm and others [4].

In deposition technology, material is delivered either in powder form or in wire feed form. Powder method is more versatile and most of the metals and ceramics are available in powdered. The powder is introduced as a toroid surrounding the laser beam which is focused to a small spot size using shielding gas flow, as illustrated in Fig 1.6.

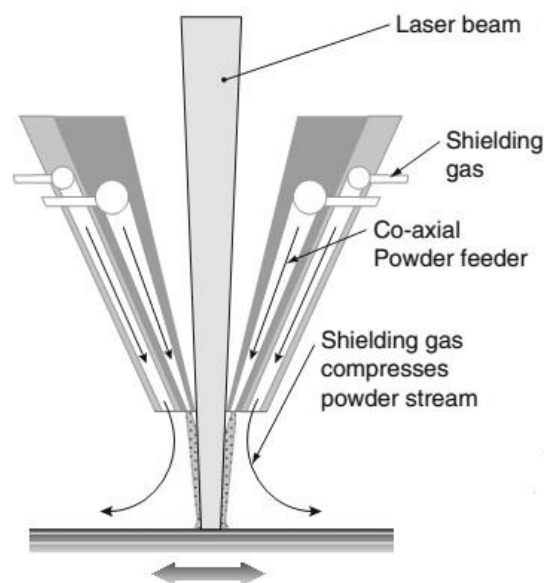


Figure 1.6: Deposition technology (LENS Process) [1]

In wire feeding, feedstock capture efficiency is 100 percent as the total energy transferred to the materials is captured in the molten pool and the total deposited volume is equal to wire utilized. This method is totally liable as the total installation cost for is quite low as a normal metal inert gas (MIG) welding system can be converted to the wired feed BD unit by integrating that to a CNC machine [7]. Weld-deposition technology using gas metal arc welding (GMAW) system is the one that we are using in IIT Hyderabad for AM of metallic objects, because of its versatility in creating functionally graded materials (FGM) and cheapness of the system. The major challenge is the formation of crack and deformation during production process. This may reduce the load carrying capacity and influence the endurance limit of the part produced. These defects occur due to the residual stress that is being formed during the process. Higher tensile stress can cause corrosion cracking of the material in the future stage. So proper heat management can reduce the residual stress distribution. This can be controlled using various weld parameters and path planning parameters such as area filling paths. Here, an attempt is made to study the influence of area filling path on the temperature gradient, thereby the residual stress.

1.2 Area Filling

In order to fill a layer using beam deposition, proper path planning is to be done for the weld torch to fill the area in the effective way. There are mainly two types of area filling paths Fig 1.7 [8 , 9]

- a) Direction-parallel area-filling
- b) Contour-parallel area-filling.

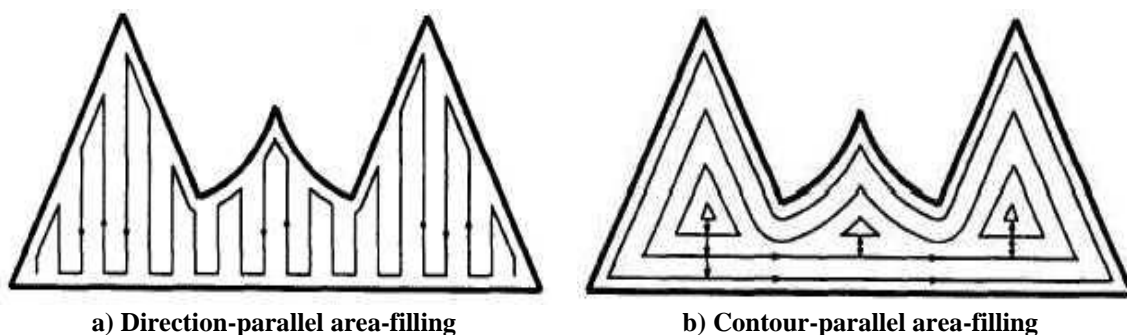


Figure 1.7: Different types of area filling methods [9]

Direction parallel filling is also known as raster filling while contour parallel is also known as vector filling or spiral filling. The fundamental difference is that in the former the path starts from one end of the area and ends at the other parallel to any of the axis of the coordinated system, slowly filling in a zigzag manner, while in later the path is parallel to the perimeter. Directional parallel area filling can be further classified as in line area filling and zigzag area filling. Inline area filling is having unidirectional paths hence it is not continuous while in zigzag, filling takes place in both directions in a continuous

path. Contour parallel area filling is of two types, outside-in contour and inside-out contour. In former the path starts from outside and fills towards inside and ends in the middle and later is just reverse of the same, that is first the center is being filled then moving to the outside perimeter as shown in Fig1.8.

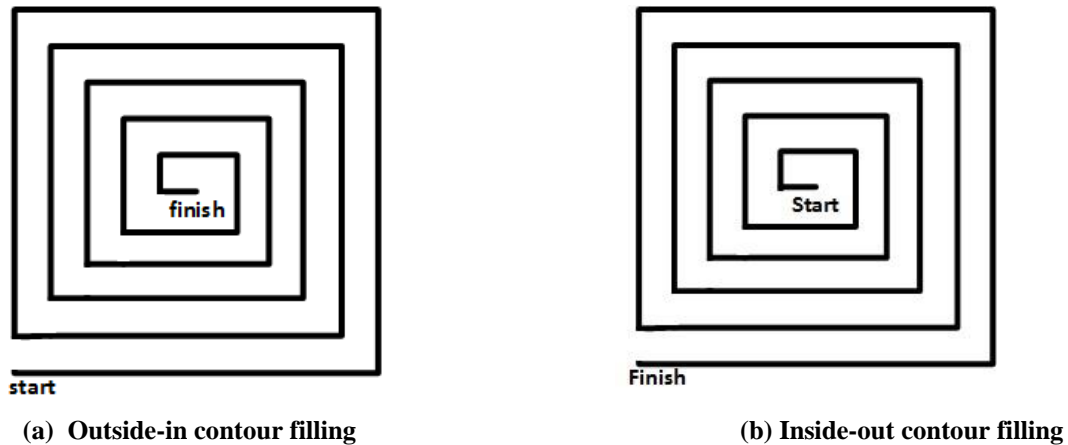


Figure 1.8: Different types of contour area filling methods [10]

1.3 Problem Definition

The main constraint in producing metallic components using additive manufacturing is the residual stress that develops during the deposition process. These residual stresses decrease the strength and create deformation in products. Such products need to undergo the post process like heat treatment, shot peening etc. Before its actual use, these processes will change the property of the part produced and thereby strength decreases further. Because of these reasons additive manufacturing is not being used for large scale production and fabrication of precise parts.

Residual stresses are the major issue in the AM process as it constraints the range of products that can be manufactured using additive manufacturing process. The post production process like heat treatment and shot peening are undesirable due to the extra time involved. So the preferred option is by reducing the residual stress in the production stage itself. Since the technology is not matured enough modeling approach can be a viable option to predict the outcome of the process. This will not only make the researcher and engineers understand the science behind the process but can easily make the process acceptable to industries.

As will be elaborated in the subsequent chapters, many numerical and statistical based modeling works has been reported regarding the formation of residual stresses in welding. But only few works has been reported in case of additive manufacturing using weld-deposition. Proper experimental and numerical

study of residual stress in beam deposition with focus on the area-filling path can reduce these issues substantially.

In this thesis, an attempt is made to develop an algorithm to model weld-deposition AM in finite element analysis using Ansys Mechanical APDL. The same was used to analyze the effect of area filling path patterns on the temperature gradient and the thermally induced residual stresses. The obtained results were then experimentally verified.

1.4 Objective of Study

- Residual stress distribution for various area-filling patterns to be modeled using FEA software ANSYS Mechanical APDL.
- Study of the influence of the area-filling path on residual stress.
- The modeling results to be verified experimentally using weld-deposition and the measurement of residual stress is being measured using X Ray Diffraction.

Chapter 2

Literature survey

2.1 Introduction

The analytical theory of heat transfer was first introduced in 1930s by Rosental [11] and it was further refined in course of time. Among those most referred one was by Rykalin [12]. The first explanation of the general theory of thermal stress was given in the work done by Boley and Weiner [13] in 1960. Later in 1980's only, the first paper defined to three dimensional heat transfer were published. And in 1988, Goldek and Bibbly [14] published computational welding mechanics, which is the base stone for all researches in this field. Different research works in computational welding and additive manufacturing processes are given in the following section.

2.2 Modeling of weld deposition for residual stress

There are a number of studies conducted on welding using finite element modeling technique for the thermally induce residual stresses on weld bead. Among those, remarkable studies are done by Kong and Kovacevic [15], Kong et.al. [16] and Deng et.al. [17]. In studies done by Kong and Kovacevic [15], investigation is done on the thermally induced stress fields during welding lap joint by GTAW process. The 3D finite element model was developed using ABQUS. The experimental validation was done by using Hybrid laser-GMAW system and the residual stress is been measured using x ray diffraction technique. The different components of residual stress obtained with respect to welding speed are compared with the experimental results. While Kong et.al. [16] Considered the hybrid laser GMAW for his experiments in which numerical and experimental study is been conducted. The paper outlines the effect of welding speed on isotherms and residual stresses on welded joints. The paper concludes that the concentration of residual stress decreases with increase in speed. While Deng et.al [7] conducted numerical analysis in ANSYS APDL of residual stress and deformation due to it during electro stag welding. And paper proves that the welding simulation results obtained using moving heat

source method shows close similarity to the experimental results and thus it can be used to find the integrity of the structure.

There are a number of parameters that influence the thermally induced residual stresses, such as weld speed, distance from the weld direction, heat input, etc. As Stamenković and Asovic [18] studied about the variation in residual stress distribution along the weld bead direction. They have studied residual stress due to manual arc welding manual in which the axial residual stress is calculated using FEM software ANSYS which is compared with that of the experimental results as shown in Fig 2.1. The paper suggested that finite element analysis can be used for other welding analysis with different parameters like, welding speed, current voltage, filler wire rate etc. Whereas Ameen et.al.[19] Studies on the relation between heat flux input and residual stress. They examined the influence of residual stress on butt weld; an experiment was performed using the TIG welding setup for different v angles such as 30°, 45°, 60°, 90°. In this paper the numerical result obtained from finite element software ANSYS Mechanical APDL is validated using experiment, and concludes with the relation between the heat flux input and residual stress. In addition to that, Sudersanan and Kempaiah [20] brought up with a comparison with heat energy input with longitudinal stress. They studied in the effect of heat input and weld speed on residual stress using finite element simulation and validated experimentally. They studied the residual stress induced in the dual phase steel with changes in heat input and travel speed during Butt welding. Multi pass butt welding is done on DP Steel specimens using MAG welding system. The residual stresses at different portions are measured using X-ray diffraction technique. The variation in longitudinal residual stress is plotted in Fig 2.1 with respect to welding speed and heat input. Nodeh et.al. [21] have developed an electro-thermo-mechanical two-dimensional FE model to predict temperature and stress fields generated after the resistance spot welding process. The accuracy of the model has been found reasonably well with the experimental results. The tensile residual stress has been found to be more at the weld center which eases down towards the nugget edge.

The study on the influence of the base plate thickness is done by Yagi et.al [22]. In this paper they have performed finite element (FE) analysis of welded sections of steel pipes. A brief survey of welding simulations has also been conducted. Two pipe thickness with different range of pipe diameters are investigated and the effect of number of beads and wall thickness of the pipes; on the residual stress formation on the welded section has been studied. Significant differences in the location of the formation of peak tensile and peak compressive stress in thin and thick welded pipes has been observed. In case of formation of residual axial and hoop stresses, in FE modeling, pipe diameter in case of thin-walled and inside the surface in case of thick walled, plays an important role. While Subramaniam et.al. [23] have developed a statistically designed experimental approach to identify the best power supply pulsing parameters required for pulsed gas metal arc welding. Fractional factorial and D-optimal method have been used to design the experiments. The developed methodology helped in reducing the dependency on power supply while considering actually pulsating condition. It also reduced the need for

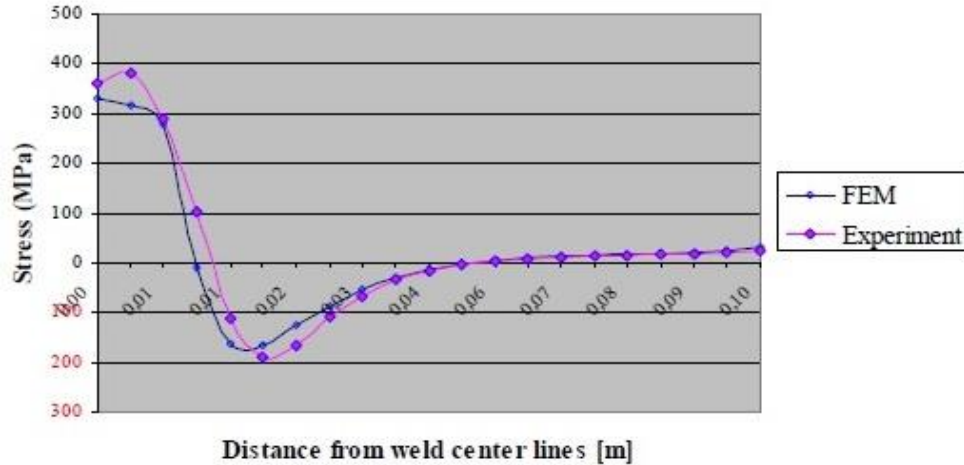


Figure 2.1: Longitudinal change in residual stress along weld bead [18]

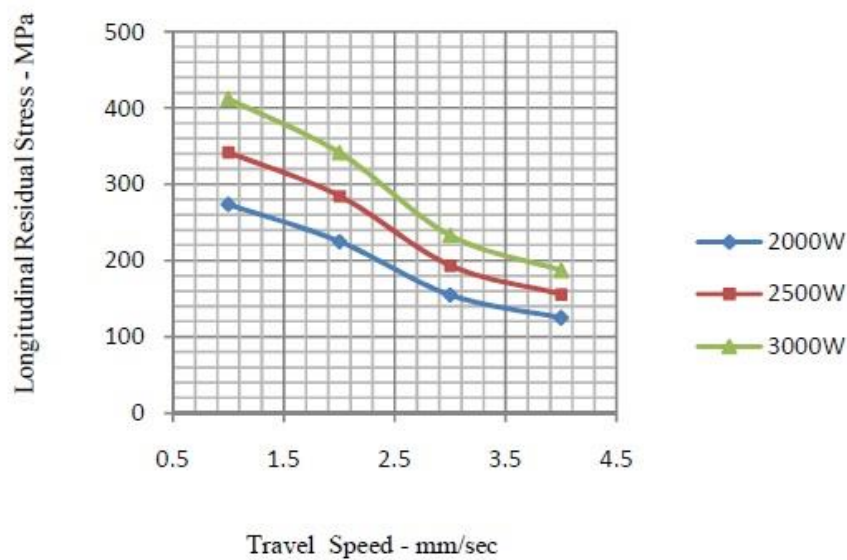


Figure 2.2: Change in residual stress with respect to welding speed [20]

conducting a number of experiments, since with the developed methodology, optimal operating region can be reached easily with minimum number of experiments. For creating a finite element model, a number of assumptions have to be followed, Babu and Kishore [24] defined assumptions, parameters and procedures that are to be followed for numerical simulation of welding. In order to obtain these results they have investigated the effect of arc welding on bead geometry using finite element simulation of hybrid welding process on 304 austenitic stainless steel.

2.3 Studies on induced residual stress during metallic AM

As discussed, thermally induced residual stress is the major challenge in metallic AM process. Number experimental and numerical research works are done in this direction. Such as the Prinz et.al [25] studied on various processing, thermal and mechanical issues in shape deposition manufacturing. They

studied the residual stress that's been induced in during creation and its potential effect like warping and debonding between layers. Effect of shot peening in issues is also been studied. Residuals stress modeling is done using FEM software ABAQUS. While Klingbeil et.al. [10] Studied on warping due to residual stress in Solid Freeform Fabrication (SFF) using weld deposition and micro casting. He compared the warping occurred due to micro casting and weld deposition using different path filling patterns. They suggested that deposition method and path planning are having great importance in reducing the residual stress. K.P. Karunakaran et.al. studied on arc hybrid layer manufacturing using Arc HLM made by the integration of MIG weld deposition equipment with CNC machine. And an economic comparison of subtractive manufacturing using CNC machining and arc HLM is done. It is stated that ArcHLM can be fitted to any CNC machine so as to form a metallic additive manufacturing system so as to convert that to wire feed weld-deposition system with lower cost.

2.4 Summary

In this chapter the history of finite element modeling of welding and its various milestones are referred. The finite element analysis can be done using number of general FEA software's such as Ansys, ABAQUS and dedicated weld modeling software's like SYSWeld, Morfeo etc. Using these packages various factors that affect the residual stress are studied and are generalized. Along with the welding process, numbers of studies are done on various issues in AM techniques in which, residual stress was found to be the major factor and various studies are done on warping mechanism due to residual stress in AM of metallic objects.

Chapter 3

Finite Element Analysis of the Deposition Pattern

3.1 Introduction

In mechanical engineering, prediction of deformation and stresses is of great concern, hence the thermal history and fluid flow is of great importance, so the numerical simulation selected should be able to handle all these physical problems. In this chapter the various governing equations that regulate the analysis of weld-deposition process has been presented. Boundary conditions are assigned so as to replicate the actual physical environment for the simulation. The methodology of the analysis process is explained in fig 3.5.

3.2 Governing Equations and Finite Element Evaluation

The weld simulation is considered as a thermo-mechanical problem in this work, hence only thermal and mechanical properties have considered, neglecting fluid flow, electromagnetism, micro structural formation etc. Hence, the equilibrium equations to be solved are only heat balance and force equilibrium for thermal and mechanical analysis. Governing equations for the analysis used in this work are explained in the following section.

3.2.1 Gaussian heat distribution

Pavelic et.al [24] proposed the ‘circular disc’ model, in which the thermal flux is in the form of Gaussian or normal distribution in the plane, the gas metal arc welding is assumed to be a double-ellipsoidal heat source as shown in the fig 3.1 [25] and it's given by

$$q(r) = q(0) e^{-Cr^2} \quad (3.1)$$

Where $q(r)$ Surface flux at radius r (W/m^2)
 $q(0)$ Maximum heat flux at the center of heat flux (W/m^2)
 C Distribution coefficient (m^2)
 r Radial distance from the center of the heat source (m)

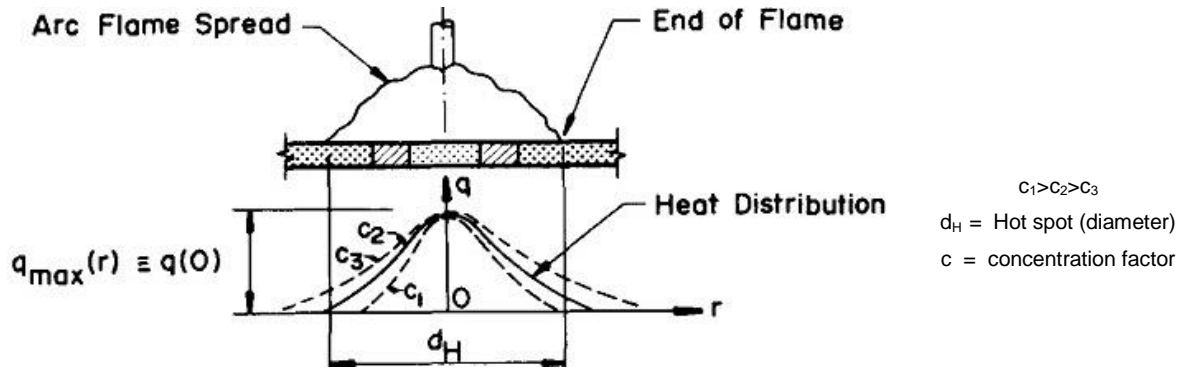


Figure 3.1: Circular disc heat source [24]

The governing equation for conservation of energy [13] is shown as follows:

$$\frac{\partial(\rho c T)}{\partial t} = \frac{\partial^2(k_m T)}{\partial x^2} + \frac{\partial^2(k_m T)}{\partial y^2} + \frac{\partial^2(k_m T)}{\partial z^2} + q_{arc}(x, y, z, t) \quad (3.2)$$

Where T Time
 ρ Material density
 C Specific heat of material
 k_m Thermal conductivity

$$k_m = \begin{cases} k_0 & T < T_1 \\ k_0 + k' & T \geq T_1 \end{cases} \quad (3.3)$$

Where k_0 Thermal conductivity of material used at room temperature
 k' Additional value by which heat transfer capability is equally considered in proposed thermal modeling
 T_1 Melting point of the material used

Here q_{arc} is the power density of the double ellipsoidal heat source which can be expressed in two components q_{arc}^f and q_{arc}^r , which gives the heat distribution of front and rear quadrants of the heat source of GMAW and is expressed as [13,25]:

$$q_{arc}^f(x, y, z, t) = \frac{6\sqrt{3}f_f P_{arc}}{abc_f \Pi \sqrt{\Pi}} \exp\left(\frac{3(x-x_0)^2}{a^2}\right) \exp\left(\frac{3(y-L_w)^2}{b^2}\right) \exp\left(\frac{3(z-v_t)^2}{c_f^2}\right) \quad (3.4)$$

$$q_{arc}^r(x, y, z, t) = \frac{6\sqrt{3}f_r P_{arc}}{abc_r \Pi \sqrt{\Pi}} \exp\left(\frac{3(x-x_0)^2}{a^2}\right) \exp\left(\frac{3(y-L_w)^2}{b^2}\right) \exp\left(\frac{3(z-v_t)^2}{c_r^2}\right) \quad (3.5)$$

Where a , b , c_f , c_r are characteristic parameters of heat sources; for normal GMAW cases values of a , b , c_f , c_r are set at 4mm, 3mm, 3mm, 7mm respectively [25], P_{arc} is the total power input which is given as

$$p_{arc} = \eta UI \quad (3.6)$$

η arc efficiency of GMAW

U voltage (V)

I current (A)

3.2.2 Assumption of finite element analysis

The following assumptions are made during the development of the finite element model:

- The work piece is initially at room temperature
- For weld modeling, it is considered that the heat source is moving with fixed Work piece
- Convection is applied to all surfaces.
- Heat loss due to radiation is ignored (it's explained in detail in the following section)
- Forced convection due to shielding gas flow is ignored.
- Only heat is transferred to the work piece, material deposition is not considered.
- Heat conduction through the clamps is ignored.

3.3 Boundary conditions

In deposition process, temperature gradient which develops elastic and plastic strains that leads to residual stresses. The heat from the deposited part is transported by conduction in the material to the boundaries. The conduction to the boundaries can be expressed in different ways which determines the

temperature gradient in the structure. The boundary conditions that are considered for thermal and mechanical analysis are explained below.

3.3.1 Thermal boundary conditions

There is mainly three boundary condition considered for thermal problems i.e. ambient temperature, convection and radiation .The boundary condition for thermal analysis for weld deposition at a single point is shown in fig 3.2. The ambient temperature is applied to the entire environment and the specimen, and it is constant value depending up on the climatic condition at the time of experiment.

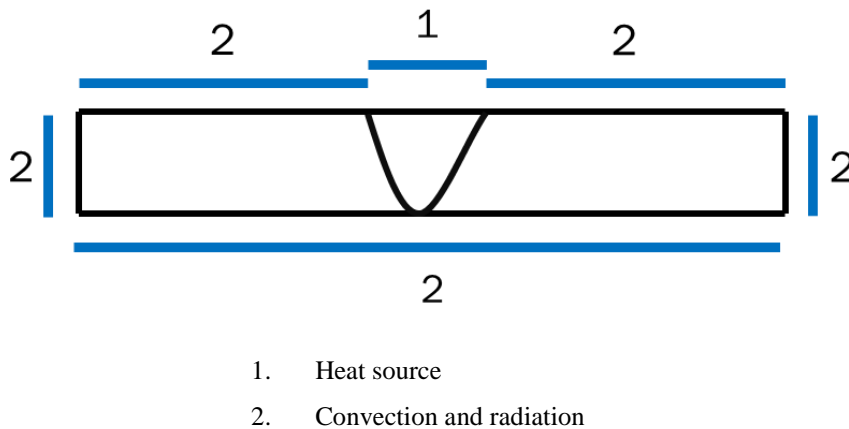


Figure 3.2: Boundary condition for thermal analysis

Heat loss due to convection is given by

$$q_c = -h_c(T_s - T_a) \quad (3.7)$$

Where h_c Heat transfer coefficient
 T_s Surface temperature of the weldment (°C).
 T_a Ambient temperature (°C)

Heat loss due to radiation is given by

$$q_r = -\varepsilon_o \sigma_o [(T_s + 273.15)^4 - (T_a + 273.15)^4] \quad (3.8)$$

Where T_s Surface temperature of the weldment (°C).
 T_a Ambient temperature(°C)
 ε_o Emissivity
 σ_o Stefan–Boltzmann constant(W/m²k⁴)

Since the value of Stefan–Boltzmann constant is of the range of 10^{-8} , so the radiation value is negligible as compared to the total value.

3.3.2 Mechanical boundary conditions

If one material is heated uniformly and has complete degree of freedom, then the body regains its original shape if it is cooled uniformly, but this does not occur in deposition process as the cooling is not uniform. The area adjacent to the recently deposited weld bead will be having higher temperature than that of other. Thereby expansion and contraction will be non-uniform, resulting in inducing stress within the body. But if the base plate is having full degree of freedom then the stress will be relieved on cooling down by deforming the base plate. But this phenomenon is not desirable so the degree of freedom all four boundaries of the plates should be constrained in all the direction as shown in fig 3.4 so that the residual stress retains inside the plate while cooling down.

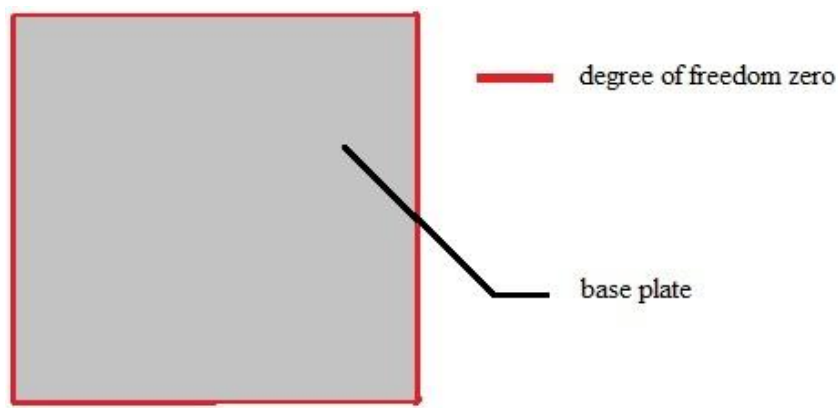


Figure 3.3: Boundary conditions for structural analysis

3.4 Process parameters used for analysis

The simulation is done on various parameters such as weld current, weld voltage, step over increment etc. which are selected based on some trials, corresponding to satisfactory weld deposition obtained, and it is discussed in detail in the next chapter.

Weld simulation is done using different area filling paths such as zigzag area filling, outside in contour area filling and inside out contour area filling which is shown in fig 3.4. The heat flux to be induced is calculated from the equation 3.1. The entire equation can be explained [25] using the distribution coefficient C i.e. If a uniform heat flux with magnitude $q(0)$ is applied in a circular area with diameter $d = 2/\sqrt{C}$, then the total heat flux input to the area is

$$q_w = \eta UI \quad (3.9)$$

Various weld parameters used for numerical analysis that is used are shown in table 3.2

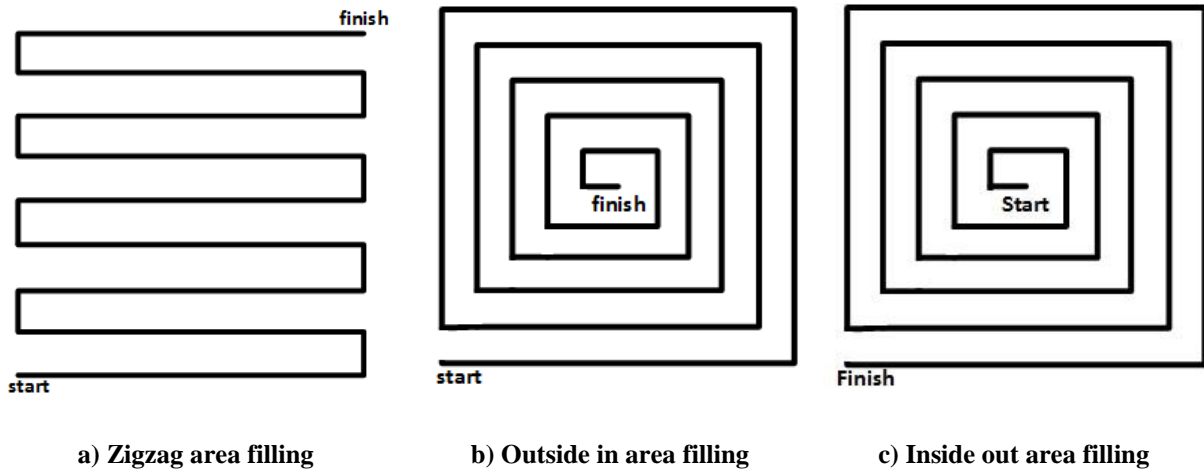


Figure 3.4: Selected area filling options for analysis

3.5 Finite element implementation of the problem in ANSYS Mechanical APDL

The process plan for welding simulation in ANSYS Mechanical APDL is given in the flowchart as shown in fig 3.5. These steps are explained in detail:

3.5.1 Selection of the element type

The type and size of element selected for the analysis is crucial for accuracy and desired process output. As the element size decreases the accuracy and processing time increases. SOLID5 is an element type available in ANSYS 13 which has 3-D magnetic, thermal, electric, piezoelectric and structural field capability with limited coupling between the fields. The element has eight nodes with up to six degrees of freedom at each node, as shown in fig 3.6. Scalar potential formulations (reduced RSP, difference DSP, or general GSP) is available for modeling magneto static fields in a static analysis. When used in structural and piezoelectric analyses, SOLID5 has large deflection and stress stiffening capabilities. Owing to these advantages finer mesh size of 1mm was chosen for the weld path as shown in fig 3.6[26].

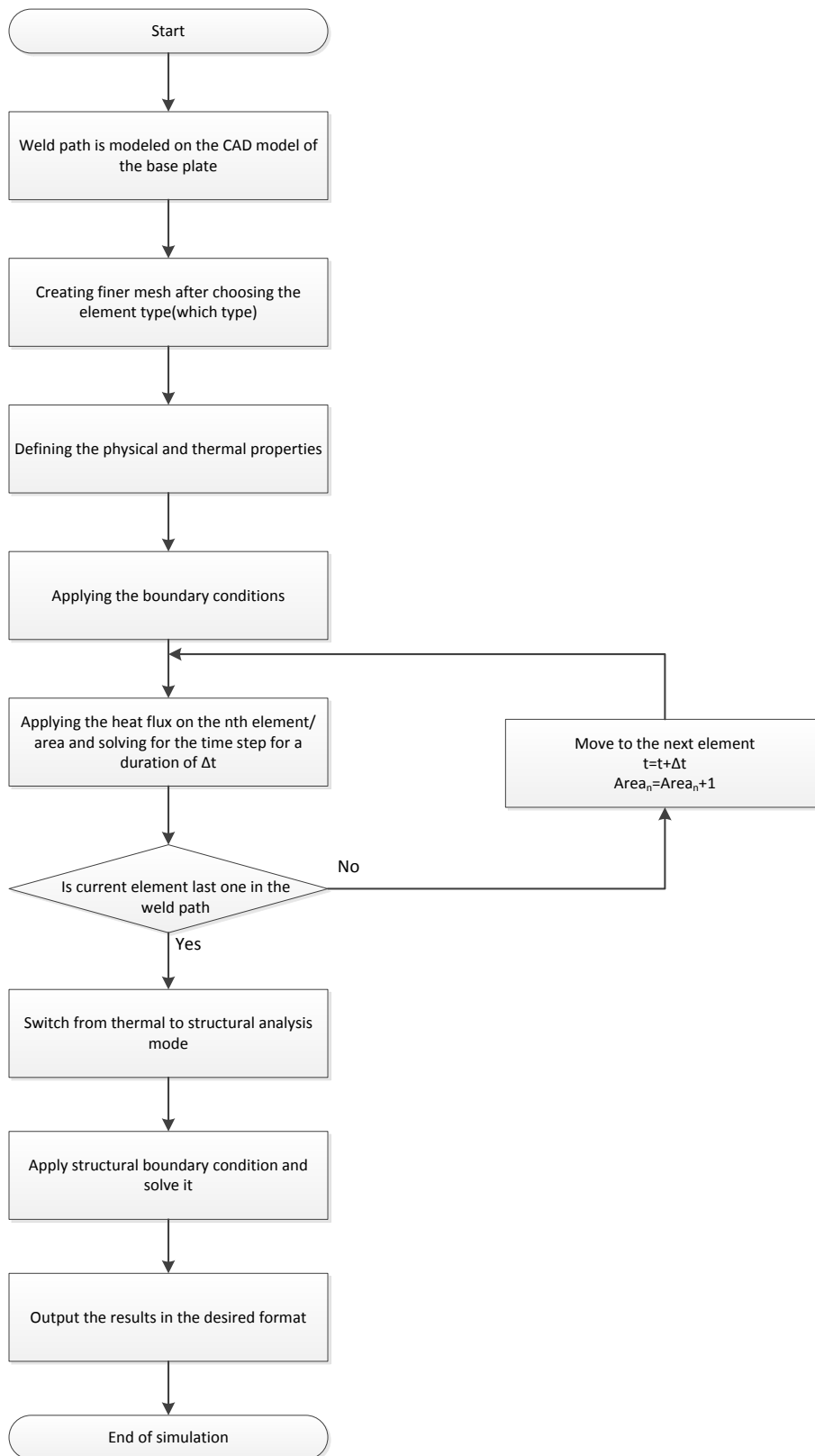
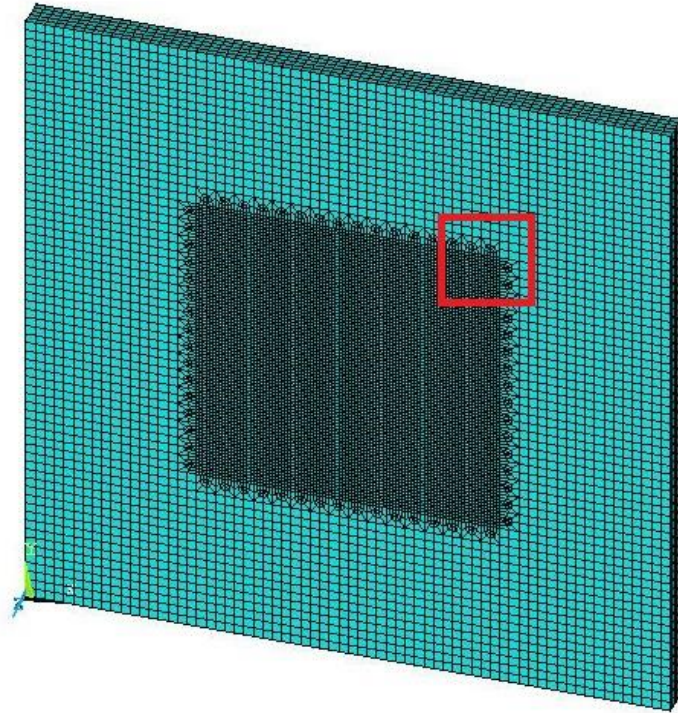
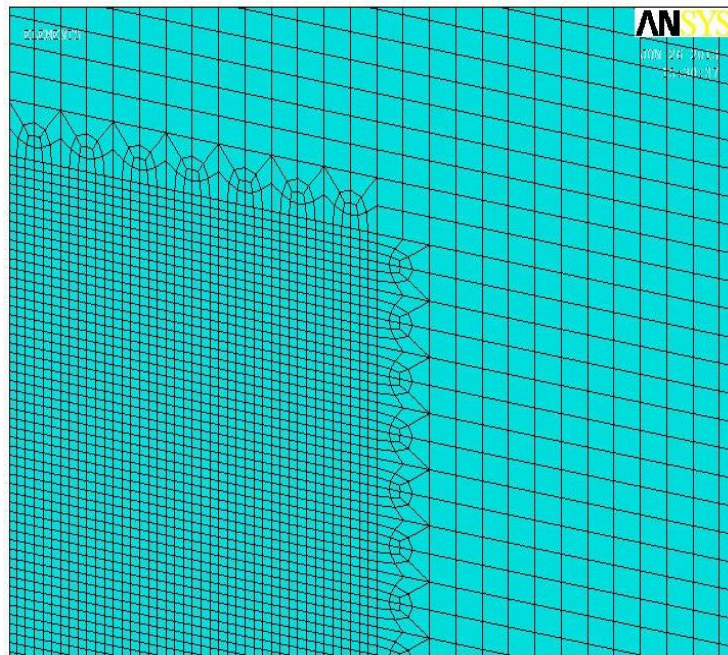


Figure 3.5: Flow chart of Analysis process plan in ANSYS APDL



a) Finite element model of the base plate and weld path



b) Zoomed view of the finite element model of weld path

Figure 3.6: Finite element model

3.5.2 Modeling of plate and weld path

Model of the plate and weld path is done using APDL codes since proper numbering of the weld path is to be done in an incremental way. So the base plate is made of cubes with size of $3 \times 3 \times 3 \text{ mm}^3$ as shown in fig 3.5.

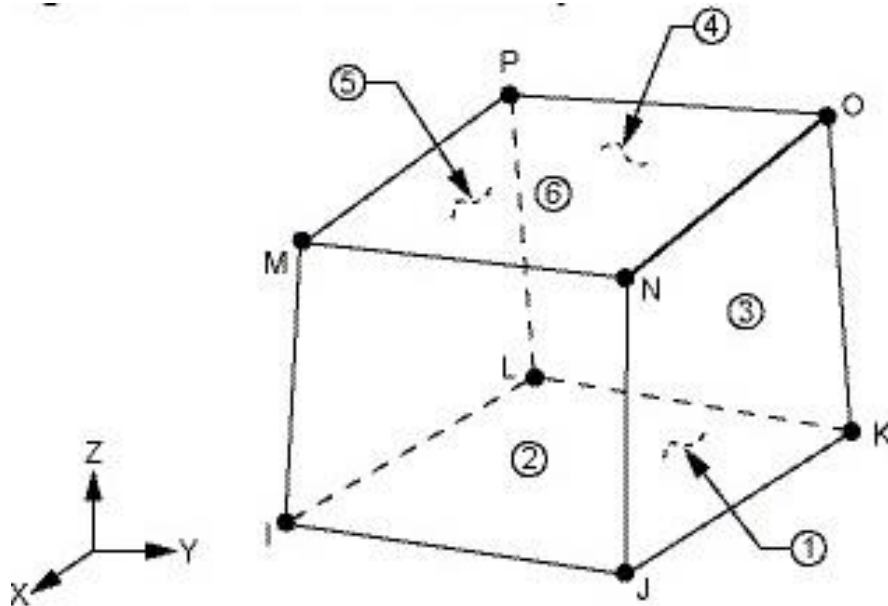


Figure 3.7: Solid 5 elements [26]

3.5.3 Material properties

The material properties of an element are controlled by the material composition. The material used in the experiments is EN08 steel. The composition of EN08 is given in table 3.1. To analyze the transient heat distribution, material properties like heat conduction, heat capacity and material density are to be considered and for structural analysis material properties such as modulus elasticity, Poisson's ratio, thermal expansion coefficient, material density are to be considered. These properties for EN08 are given in Table 3.2 and are illustrated in fig 3.7.

Table 3.1: Chemical composition of EN08 Steel

Element	Content
Carbon	0.36-0.44%
Silicon	0.10-0.40%
Manganese	0.60-1.00%
Sulphur	0.050 %
Phosphorus	0.050 %

Table 3.2: Material properties of EN08

Temperature (°C)	Thermal Conductivity (Wm ⁻¹ °C ⁻¹)	Specific Heat (J kg ⁻¹ °C ⁻¹)	Density (Kgm ⁻³)	Coefficient Of Thermal Expansion (10 ⁻⁵ /°C)	Modulus Of Elasticity (GPa)
0	480	60	7880	1.15	210
100	500	50	7880	1.2	200
200	520	45	7800	1.3	200
400	650	38	7760	1.42	170
600	750	30	7760	1.45	80
800	1000	25	7520	1.45	35
1000	1200	26	7390	1.45	20
1200	1400	28	7300	1.45	15
1400	1600	37	7250	1.45	10
1500	1700	37	7180	1.45	10

3.5.4 Application of Heat Flux

Gaussian heat flux is applied to the selected area. The heat flux is calculated using the equation 3.6 and is applied all nodes in the corresponding area and the load step is calculated as follows

$$t_h = \frac{L_w}{n s_w} \quad (3.10)$$

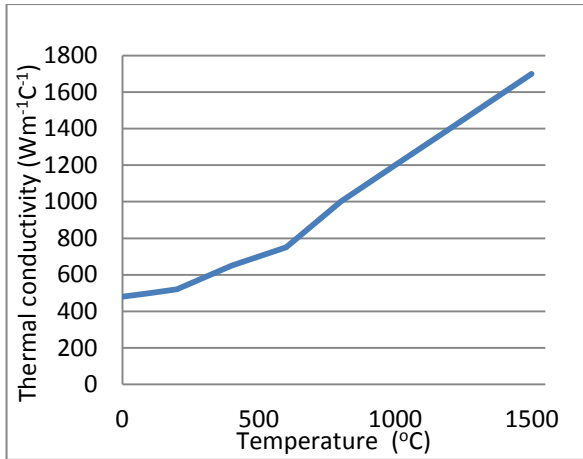
Where L_w Weld length in particular direction

n no of elements

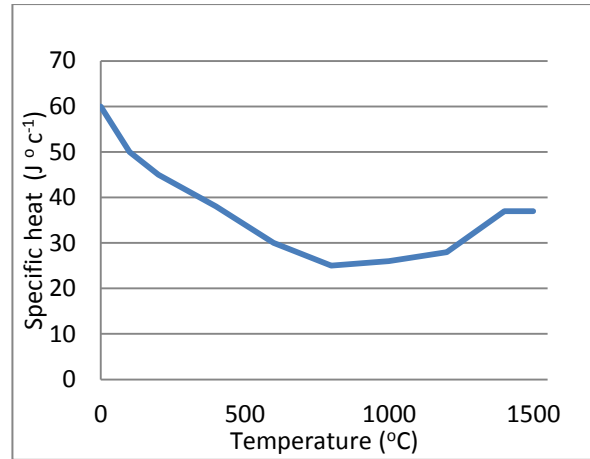
s_w Welding speed

3.5.5 Iteration of the results for subsequent element

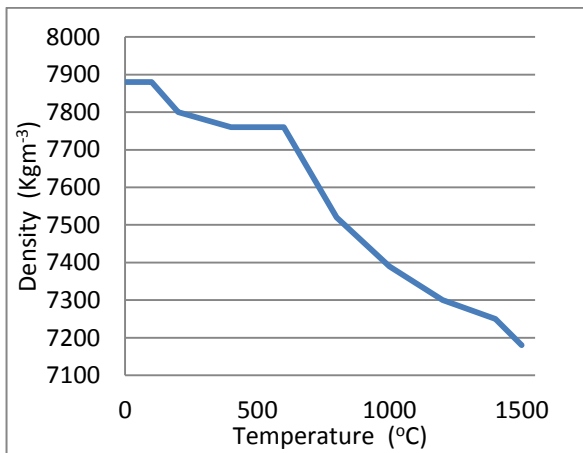
Then the model is solved for thermal results i.e. for temperature gradient. And the above steps are continued till the last area in weld path is simulated and solved. Then the cumulative heat gradient result is the exported for structural analysis. And it is solved to get the structural results i.e. residual stresses.



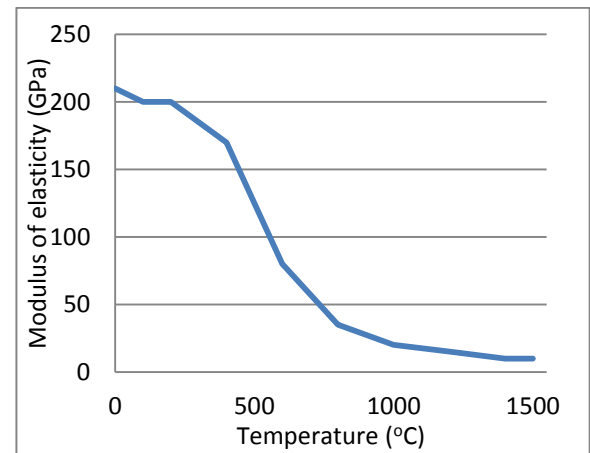
a) Thermal conductivity



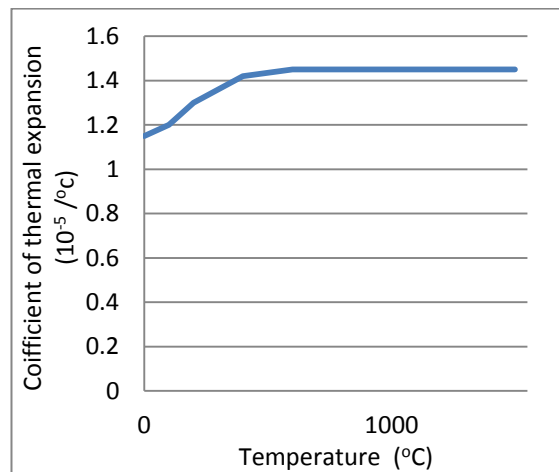
b) Specific Heat



c) Density



d) Modulus of elasticity



e) Coefficient of thermal expansion

Figure 3.8: Properties of EN08 as a function of temperature

3.6 Simulation Results

The temperature gradient on base plate heat flux input due to the weld torch model is obtained for different patterns and the residual stress that was created due to this gradient is also obtained in the contour format. The plots obtained for different formats are explained in detail :

3.6.1 Zigzag area filling pattern:

The plots obtained for the zigzag area filling pattern are shown in fig 3.8 .Figure 3.8 (a) shows that the temperature gradient obtained is not uniform and a sudden change is found at the termination point of the weld.

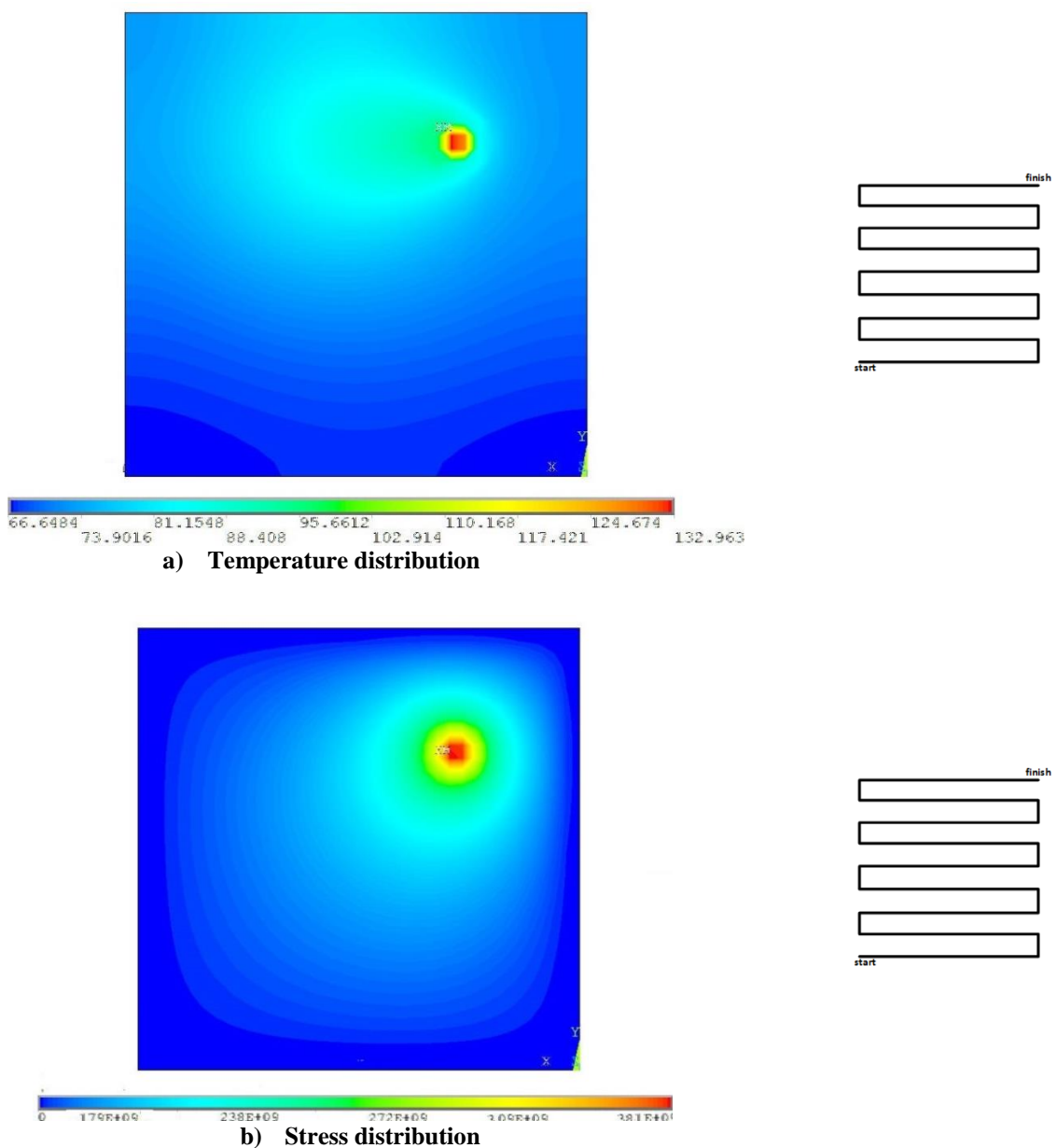


Figure 3.9: Zigzag area filling path pattern along with the path

And after that the temperature changes gradually towards rest of the weld region with termination point as center. The residual stress distribution is also in the similar way with higher residual stress at maximum temperature point and varies with respect to the temperature gradient.

3.6.2 Inside out contour area filling pattern:

Figure 3.9 (a) shows the temperature gradient due to inside out contour is not uniformly distributed, as the end point of weld is located at the corner. The maximum temperature is accumulated near to the

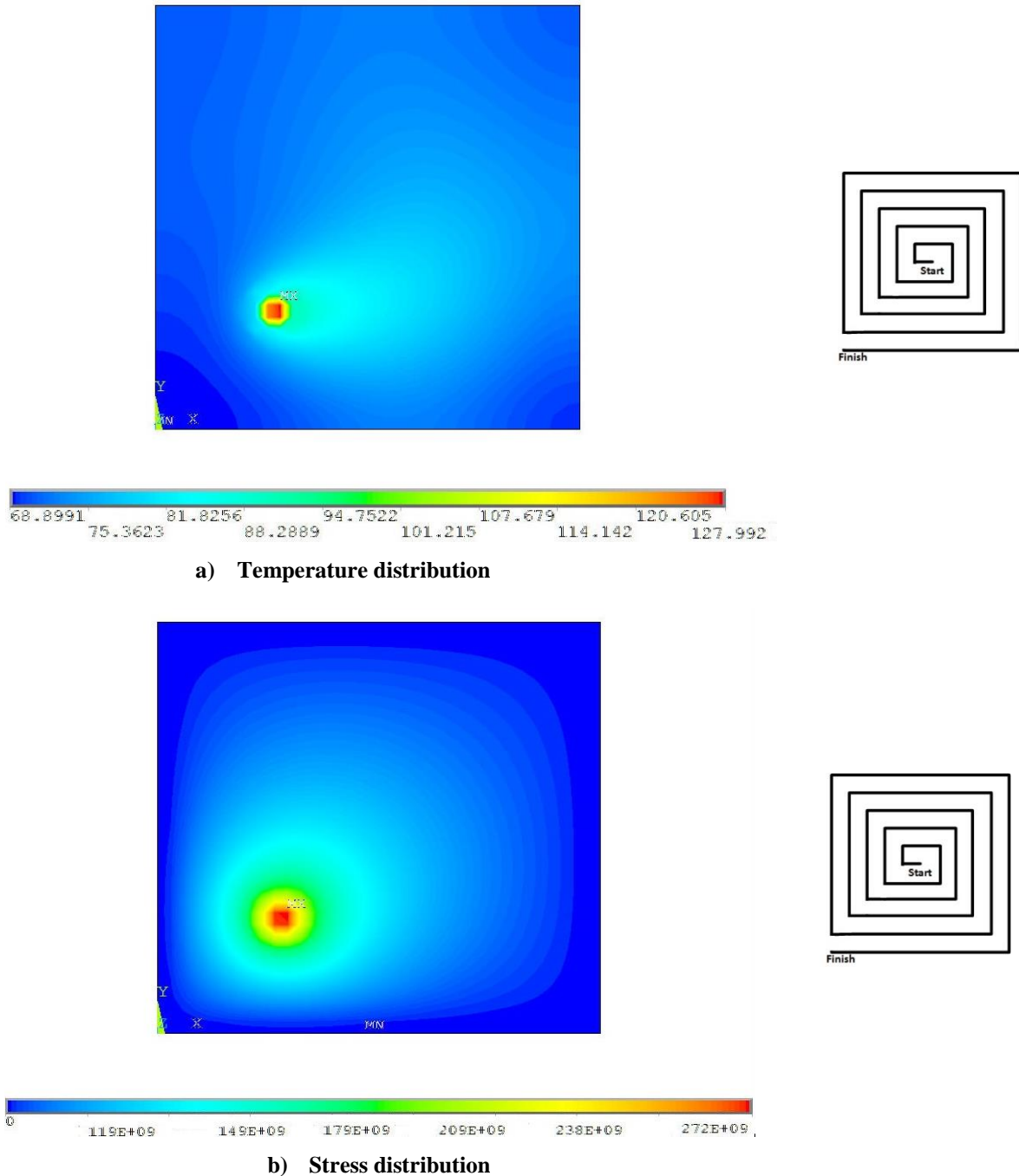


Figure 3.10: Inside-out contour area filling path pattern along with the path

final path of the weld plate. As expected residual stress distribution varies with respect to the temperature and minimum stress is found near to the base plate boundaries and maximum on final weld bead area, as shown in fig 3.9 (b).

3.6.3 Outside in contour area filling pattern

In this pattern the temperature gradient is uniform throughout the plate with respect to the center but it found that the maximum temperature accumulated is at the center and it is much higher than the

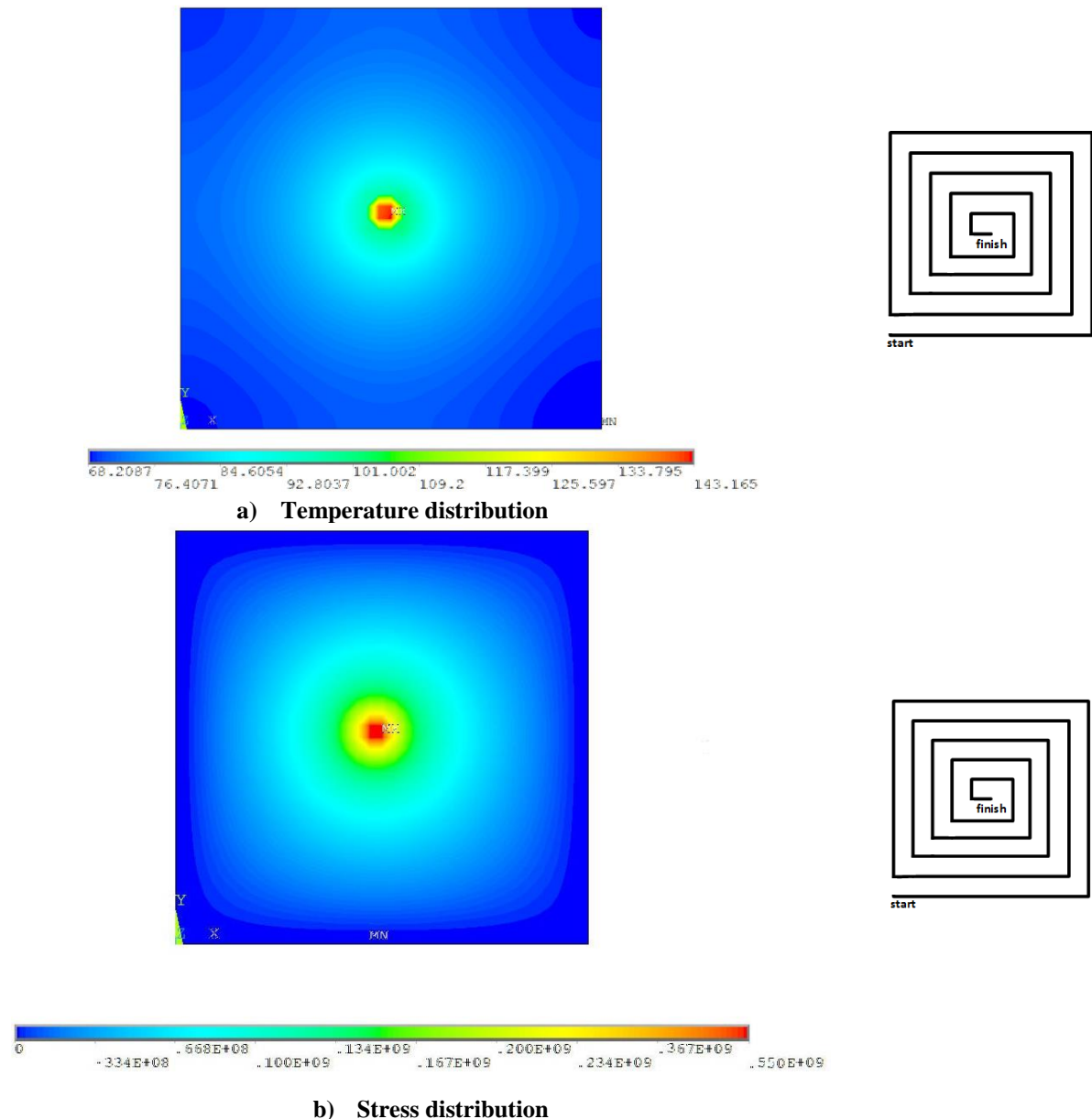


Figure 3.10: Outside-in contour area filling path pattern along with the path

Temperature obtained in the other two areas filling path operation. in this model the residual stress obtained at the Midpoint is much higher as compared to the previous paths but it's found that the residual stress distribution is uniform.

3.7 Summary

In this chapter, the numerical simulation of the deposition done using Ansys APDL is described in detail. The application of physical conditions to the finite element model has discussed and the implementation algorithm has presented. The simulation results obtained are compared to the experimental results in the subsequent chapter.

Chapter 4

Experimental Validation

4.1 Introduction

In this chapter, the results obtained using finite element analysis are verified experimentally. The first attempt is to determine the parameters that are to be followed for simulation and experimental analysis. For that number of trial runs are conducted by varying deposition parameters. Later using these parameter experiments are done with pre-planned experimental setup. And finally the results obtained are compared with the simulation results.

4.2 Initial trials for determining the operatable welding parameters

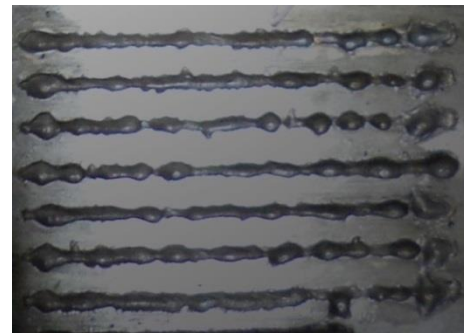
It is required to determine the various parameters of weld deposition before conducting the actual experiment. As these results are to be used for finite element analysis and for experimental validation. The parameters that are to be determined are welding current, step over increment, inert gas flow rate and torch speed. Numbers of trials are done using different values of these parameters and using combination of two or more parameters to get a decent weld. Ultimately, trials are done using these parameters on actual area filling paths.

Trials by changing weld parameters for single straight bead using twin wire welding system mounted. In Initial trials done weld speed is varied from .5m/min to 3m/min for different current values ranging from current 80A to 160 A, the results from those are shown in fig 4.1. Figure 4.1 (a) and Fig 4.1 (b) shown the weld bead obtained for 80A and 110A, where the weld bead is not continuing with non-uniform thickness for the entire range of torch speed from .5m/min to 3 m/min. Figure 4.1 (c) shown the weld deposition obtained using the current 120A in which decent weld is obtained very low weld speeds, but we can do weld deposition at such low speeds since the heat accumulation will be very high which can even cause cracks in the plate. In fig 4.1 (d) shows 130A weld beads with reasonable decent deposition at torch speed of 2 m/min which can be accepted. Figure 4.1 (e), fig 4.1 (f) and fig 4.1 (g) shows weld beads obtained using current 140A, 150 A and 160A weld depositions respectively

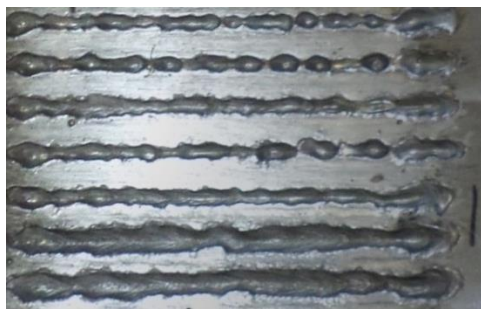
in which it is established that deposition rate increases with the current. The weld bead quality also increases with current, that is not remarkable as compared to the total energy input, as the thermal gradient increases with the energy input which in turn induces the thermally induced stresses [1,2].



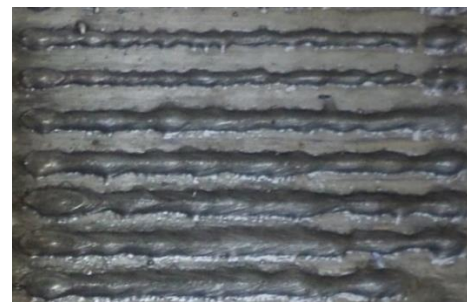
a) 80A



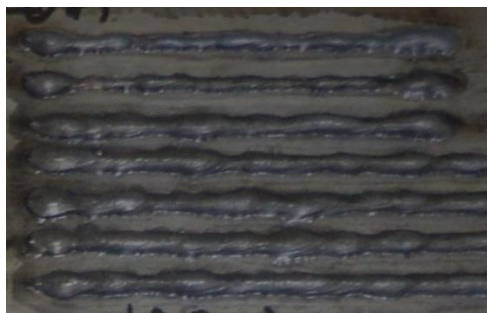
b) 110A



c) 120A



d) 130A



e) 140A



f) 150A

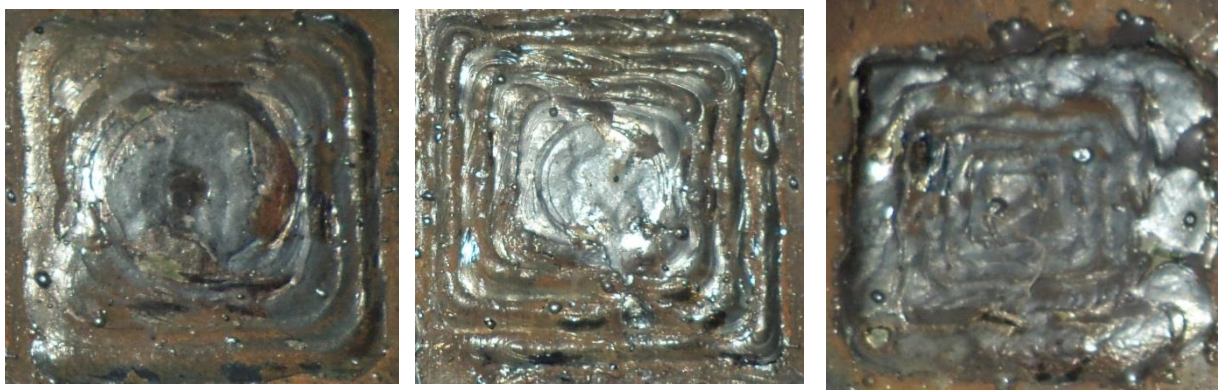


g) 160A

Figure 4.1: Weld beads obtained for different welding currents with weld speeds ranging from .5m/min to 3m/min

After conducting trials on straight weld paths, the platform is shifted to area filling weld path in which number of trials are conducted using GMAW station mounted on CNC machining Centre. Weld deposition is done each area filling path patterns by changing parameter such as weld speed, weld current, and step over increment. Figure 4.2 shows various trials done using the Step over increment 5mm and fig 4.3 shown various attempts done using the step over increment 3mm. Here “I” represents the input current (amp) and “S” represents torch speed (m/min).

Figure 4.2 shows that In weld deposition area with step over increment 5mm the, total area was not covered with uniform weld height, hence this parameter cannot be adopted for the experiment. Fig 4.3 owes that the path filling operation with increment 3mm increases the chance to fill the entire area for all selected patterns and it gives a decent weld over the pattern here speed is varied from .4m/min to 2m/min and the current is varied from 90A to 130 A.

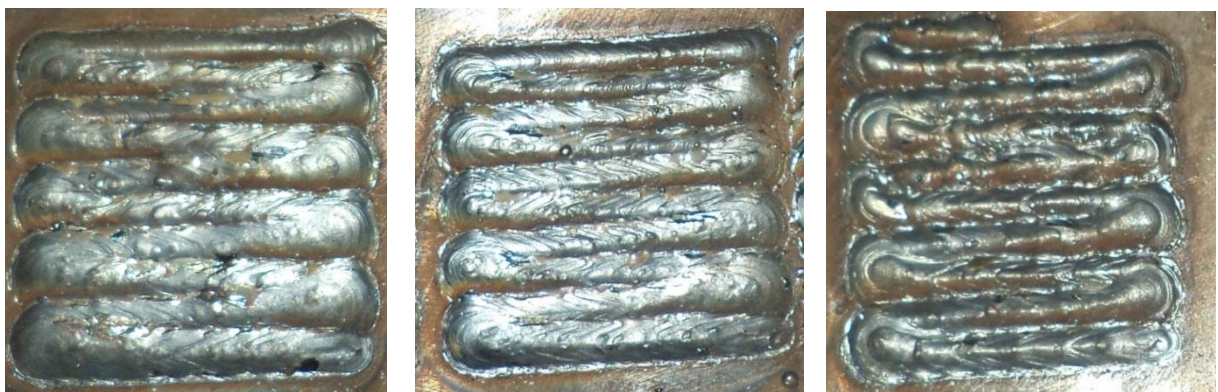


I=130A, S=. 5m/min

I=90A, S=1.5m/min

I=120A, S=.75m/min

a) With step over increment 5 mm contour path



I=90A, S=.4m/min

I=90A, S=1m/min

I=90A, S=2m/min

b) With an increment 5mm zig zag path

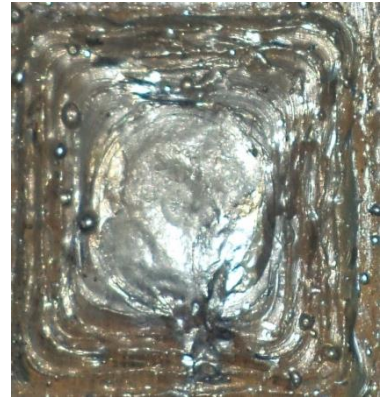
Figure 4.2: Deposition patterns obtained with step over increment 5mm



a) I=130 A, S=1m/min, IO



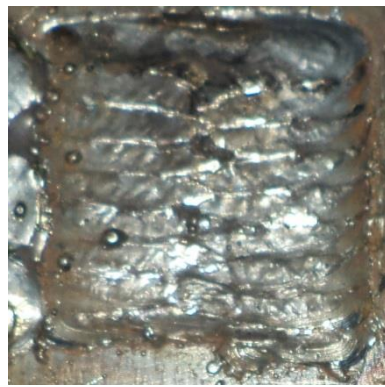
b) I=120A, S=.4m/min, OI



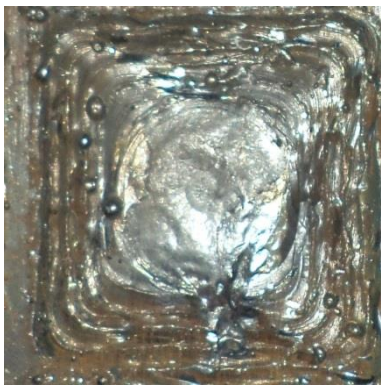
c) I=120A, S=1m/min, OI



d) I=130A, S=.4m/min, IO



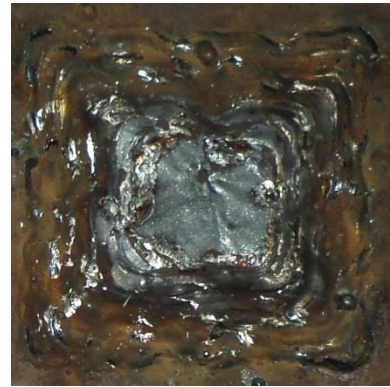
e) I=130A, S=1m/min, ZZ



f) I=130A, S=1.5m/min, OI



g) I=130A, S=2m/min, ZZ



h) I=130A, S=2m/min, OI

Figure 4.3: Deposition patterns obtained using stopover increment 3mm

4.3 Experimental setup

The entire experiment is done using GMAW using inert gas argon for the shielding purpose. The experimental setup consists of three sections.

- 1) Fixture
- 2) Weld-deposition system
- 3) Residual stress measurement setup.

These are explained in detail in the following section:

4.3.1 Fixture Design

During experiment, if the specimen is allowed to cool down with full degree of freedom then the residual stress induced within the material will try to relieve by deforming the base plate, this condition is not desirable hence fixture is to be designed in order to retain the stress. The considerations that are to be done for fixture design are:

- 1) Equal and uniform force should be exerted throughout the boundary of the plate.
- 2) Proper clearance should be provided for the movement of the weld torch and for the movement of the XRD probe for residual stress measurement.
- 3) Deposited area of the base plate and its bottom surface should not be in any contact with any other material (i.e. Heat loss is through convection only)
- 4) The fixture should withstand the force exerted due to the induced residual stress.

Fixture consists of two hollowed square plates which sandwiches the workpiece and is tightened using eight align screws .The fixture design is shown in fig 4.4 and fig 4.5 shows different views of the fixture.

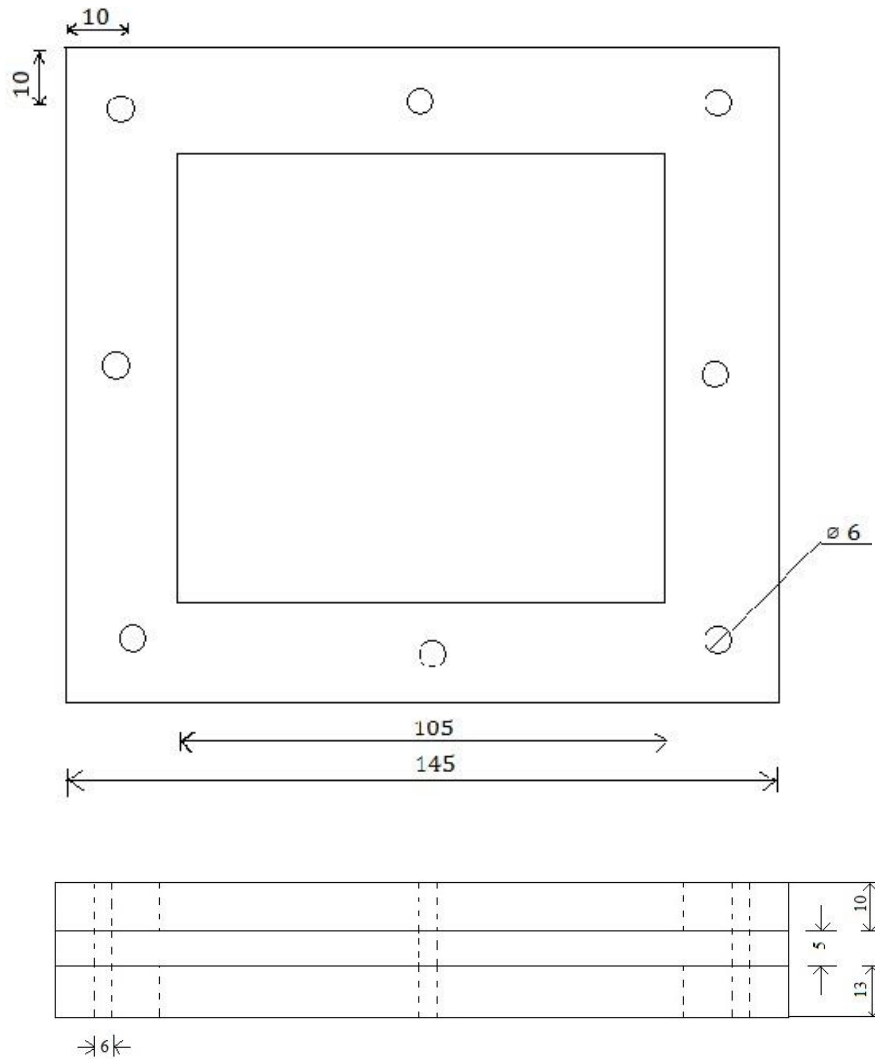
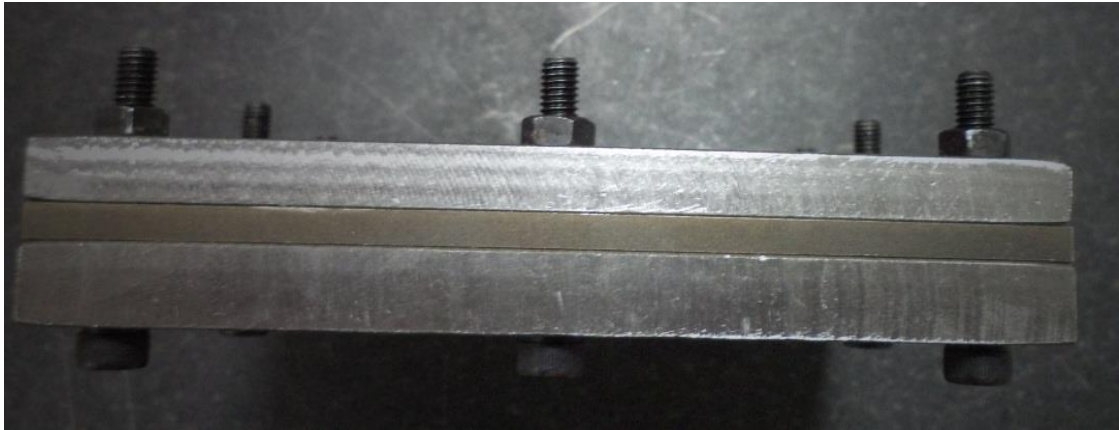


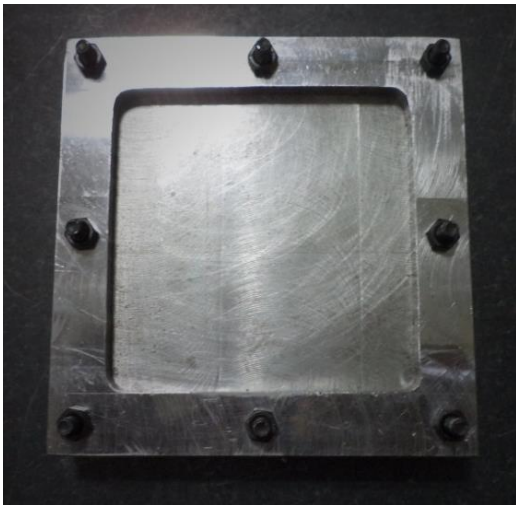
Figure 4.4: Fixture design

4.3.2 Weld-Deposition system

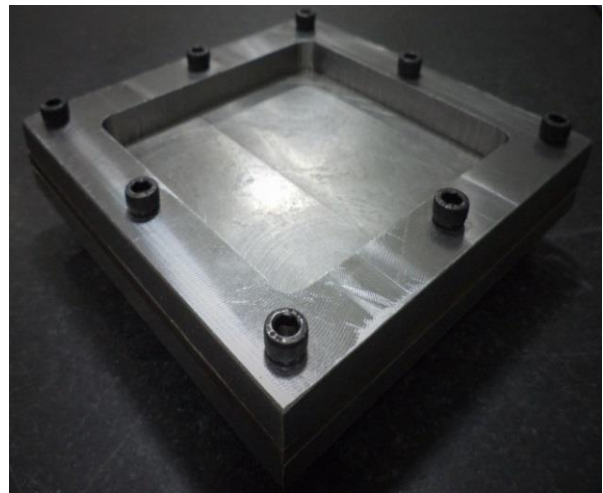
The deposition process that we use in IIT Hyderabad is a weld base deposition method, which is made by the connecting a GMAW system to a CNC machine [3]. The machine used for this purpose is AGNI BVM 40 TC20 vertical machining center with Fanuc controller as shown in fig 4.5. This machine has 3 axes of motion, i.e. X, Y, Z. Where X and Y axis motion is achieved by moving the fixture table and Z axis by tool post. The GMAW station used is EVM Taurus 551 synergic GMAW system shown in fig 4.6. For converting this system to a weld arc based deposition system, the weld torch is attached to the tool holder of the CNC machine so as to replicate the movement of the tool as in a CNC machining center as shown in fig 4.7. Switching on and off of the GMAW system is done manually.



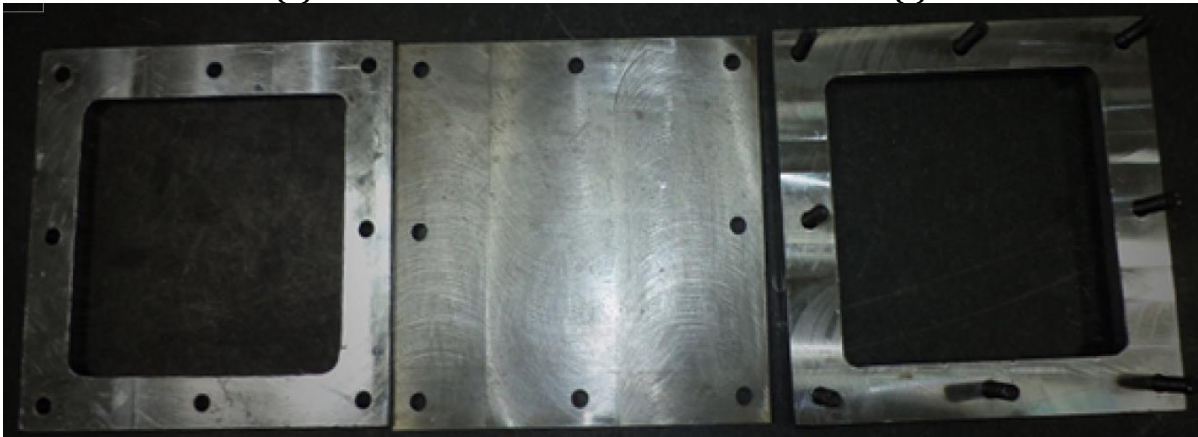
(a)



(b)



(c)



(d)

Figure 4.5: Fixture to retain residual stress of the base plate a) side view of the assembled fixture b) Top view of the fixture c) Isometric view from the bottom d) Fixture and base plate disassembled



Figure 4.6 : AGNI BVM 40 TC20 vertical machining center with Fanuc controller



Figure 4.7: EVM Taurus 551 synergic GMAW system

4.3.3 Residual stress measurement system

Residual stress is measured using proto XRD residuals stress measuring instrument shown in fig 4.8, which uses x-ray diffraction technique to measure the residual stress. The beta angle assigned for this measurement is 20° and the properties assigned are of ferrous materials. Total number of points selected for measuring residual stress is 40 over a length of 80mm.



Figure 4.8: Retro fitment on CNC machine

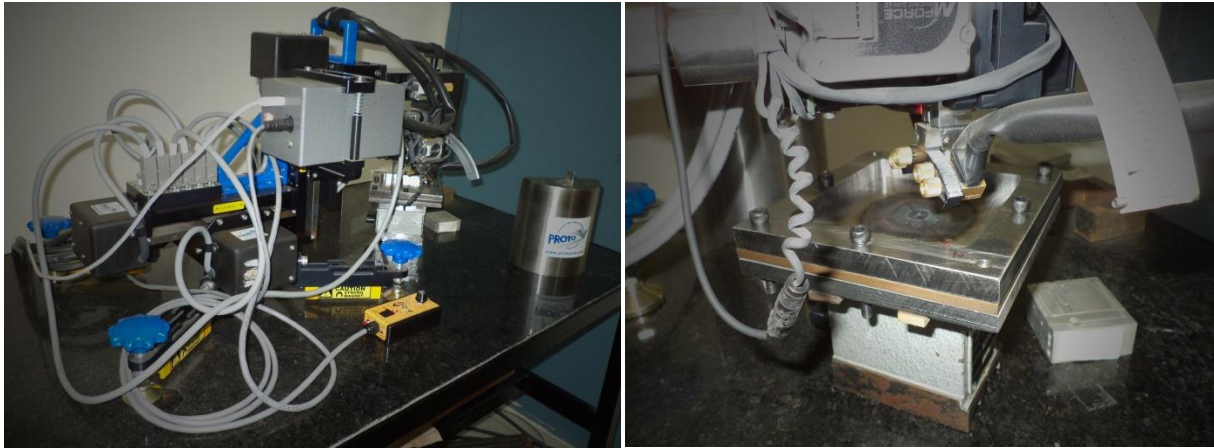


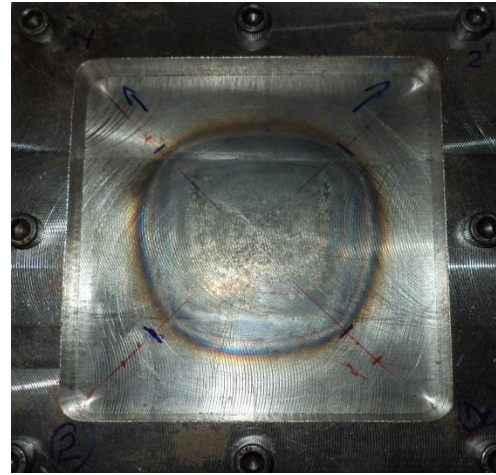
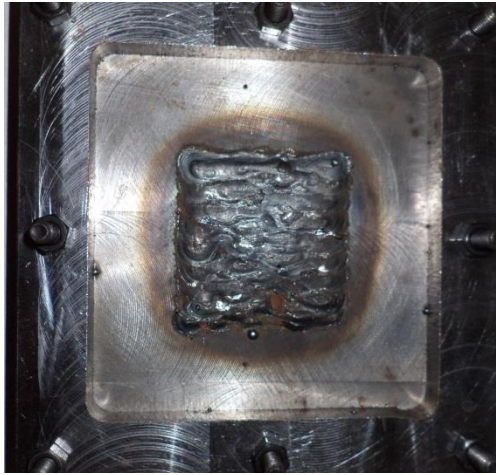
Figure 4.9: proto x ray residual stress measurement instrument

4.4 experimental procedures

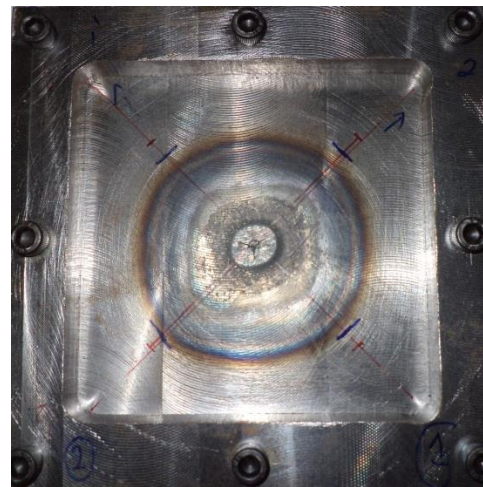
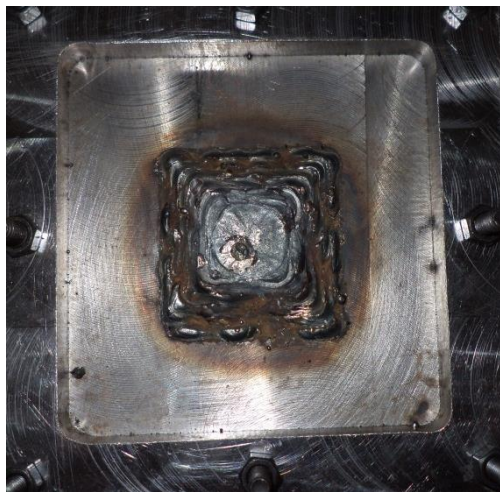
The various process parameters for the deposition process obtained from trial experiments conducted in section 4.2 are given in table 4.1 using these parameters deposition is done on plates in three different paths 1) zig zag raster area filling path, 2) inside out contour area filling path and 3) outside in contour area filling paths. The base plate is OD dimension 145 x 145 mm² in which after its being assembled in fixture the total surface area left will be 105 x 105 mm² in that after giving enough space for torch movement area filling weld deposition is done on 50 x 50 mm². Weld deposition in the above mentioned area filling paths are shown in fig 4.9. The results obtained are discussed in the following section.

Table 4.1 parameters used for GMAW

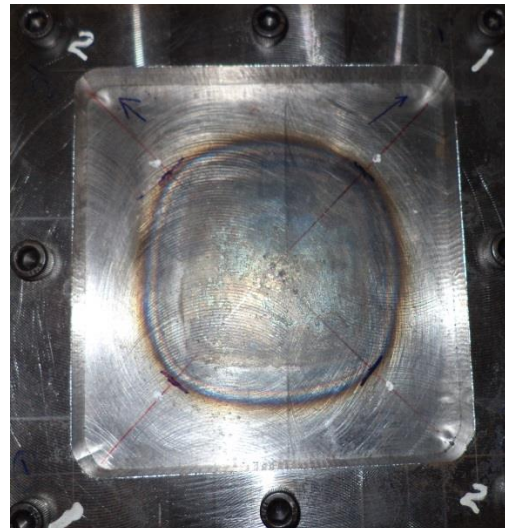
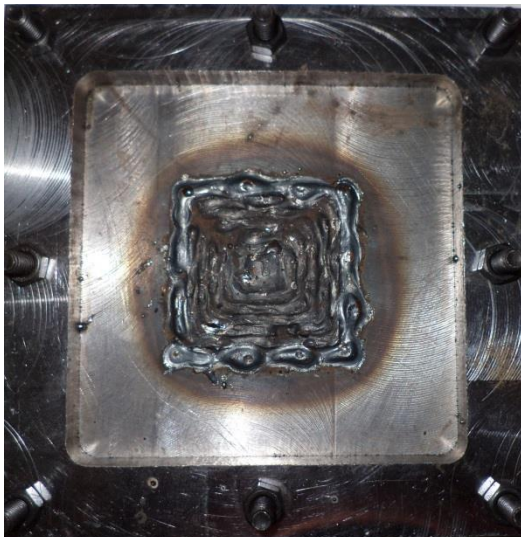
Parameter	Description
Current	130 A
Inert gas	<i>Argon</i>
Nozzle gap	15 mm
Filler material used	Copper coated mild steel wire (ER70S6)
Filler wire diameter	1.2 mm
Gas flow rate	10 l/min
Weld torch speed	2.0 m/min
Step over increment	3 mm



a) Zigzag area filling pattern



b) Outside-in contour area filling pattern



c) Inside-out contour area filling pattern

Figure 4.10: Different area filling patterns specimens

The residual stress is measured using proto XRD residual stress measurement instrument. The residual stress is measured diagonally on the bottom side specimen plate to study the induced residual stress as shown in fig 4.10. And the results obtained are explained in detail in the following section.

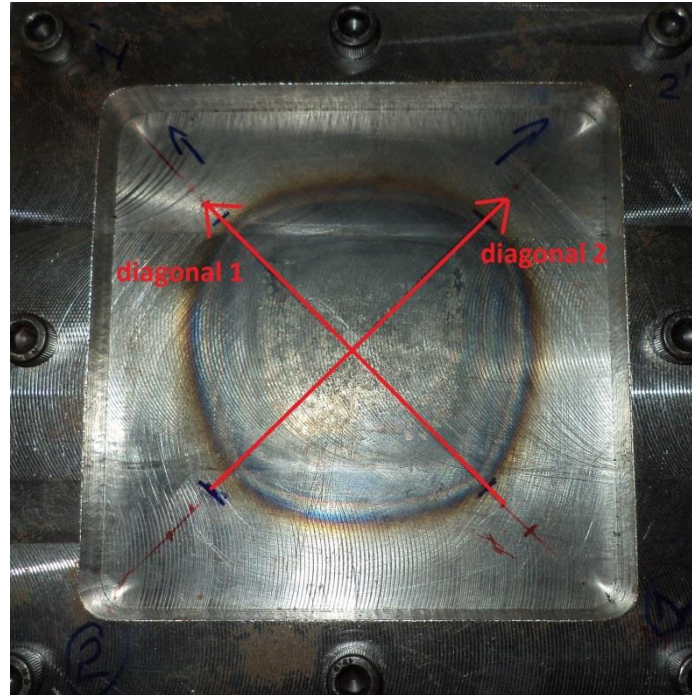
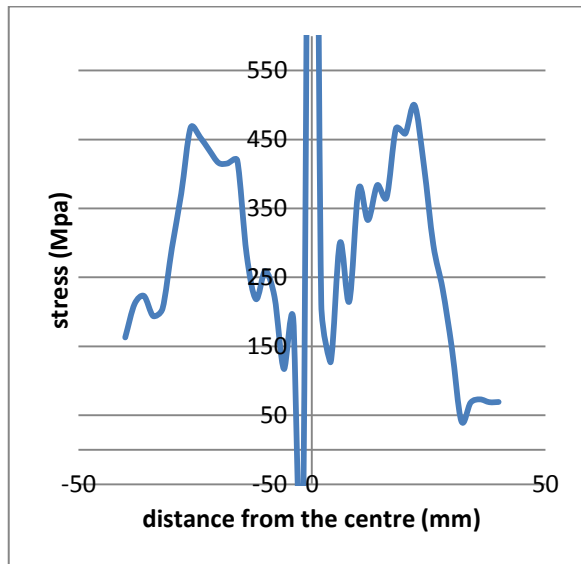


Figure 4.11: Direction of measurement in XRD

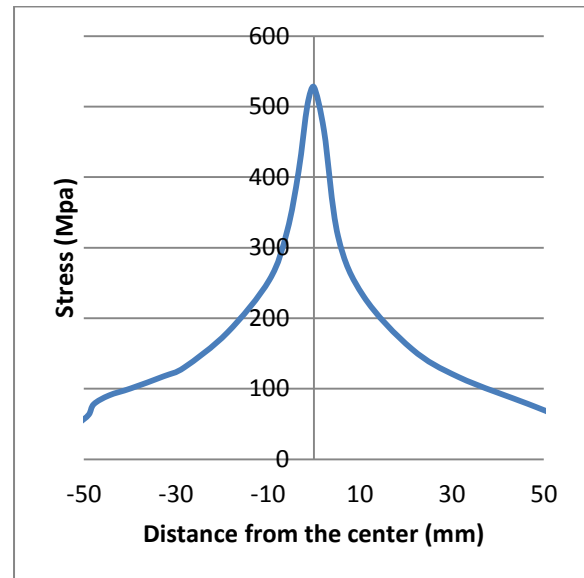
4.5 Comparison of Experimental and Modeling results

In this section numerical results are compared with experimental results for different area filling path patterns. Figure 4.12 shows the stress distribution obtained from outside-in contour area filling path pattern; fig 4.12 (a) plots the result obtained experimentally and fig 4.12 (b) plots the results obtained using ANSYS software. Both the graphs show a similar pattern in the beginning stage. Around the midpoint, it is found that the experimental values drops suddenly; simulation results on the other hand keep on increasing. This deviation is due to the formation of a crack in this area as shown in fig 4.13 , happening because the total residual stress created is more than the ultimate strength of the material. Due to the formation of the crack, stresses are relieved resulting in the formation of a valley along the center of the stress plot. Figure 4.14 plots residual stresses obtained from inside-out contour area filling path pattern. In both experimental and simulation results shown in figs 4.15 (a) and (b), the maximum residual stress is induced at the point where welding path terminates. It is also observed that the residual stress gradually decreases across the welded portion and drops to near zero around the clamping area. The results obtained from zigzag area filling pattern shown in fig 4.15 displays general similarities to that of contour form with respect to the temperature gradient. Zigzag area

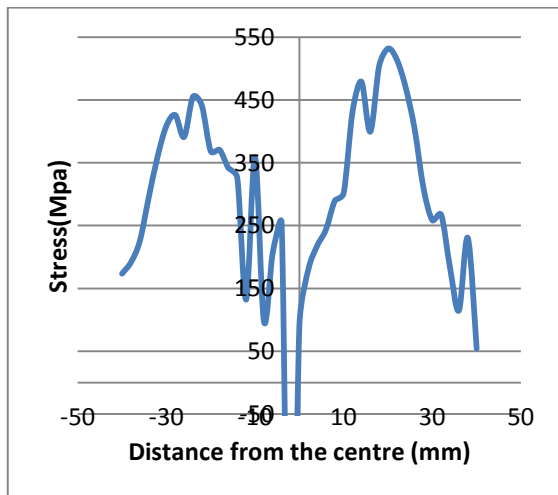
filling path's stress plot also confirms that the distribution of residual stress is maximized on the final bead and it reduces in a uniform manner towards the clamping portion.



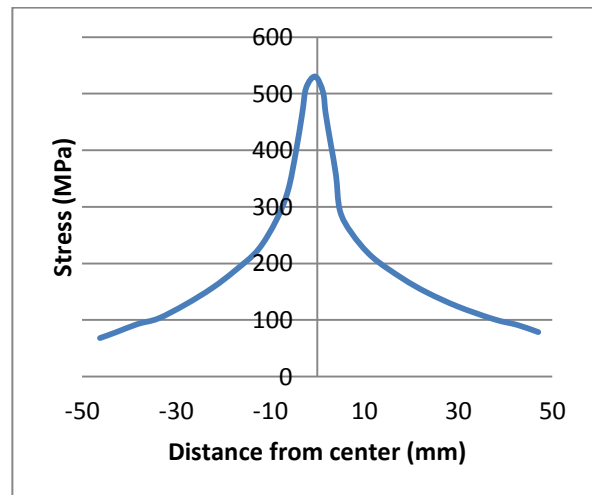
a) Experimental results for diagonal 1



b) Simulation result for diagonal 1



a) Experimental result for diagonal 2



b) Simulation result for diagonal 2

Figure 4.12 Stress distribution on the outside in contour area filling path

While comparing the experimental results and simulation results the major variations that come into notice are the fluctuation in the experimental plots and difference in the range of residual stress. The fluctuation that has observed in experimental plot may be due to the following reasons:

- The type of metal transfer in weld deposition was globular transfer so that the deposition was not continues.

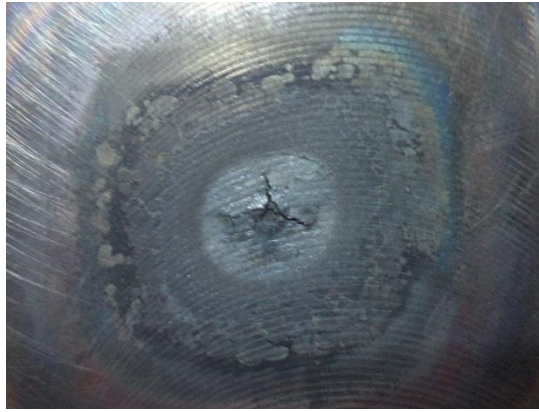
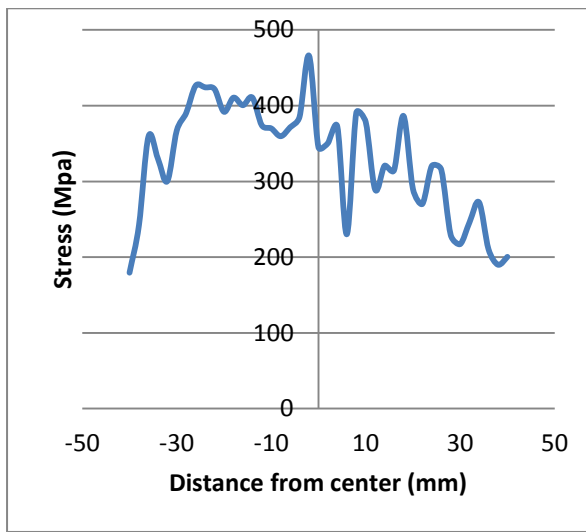
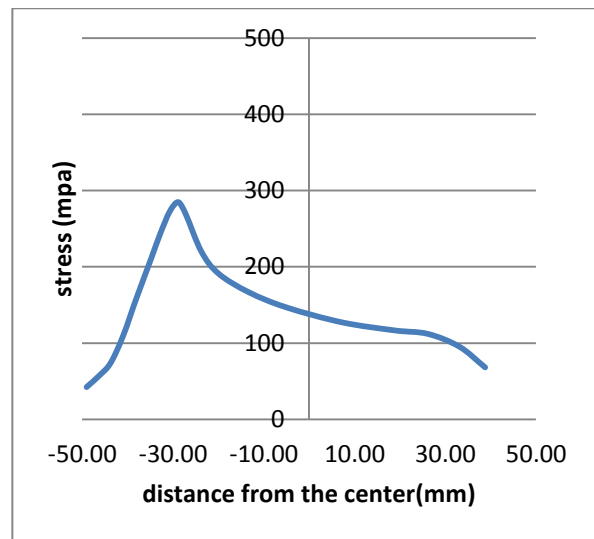


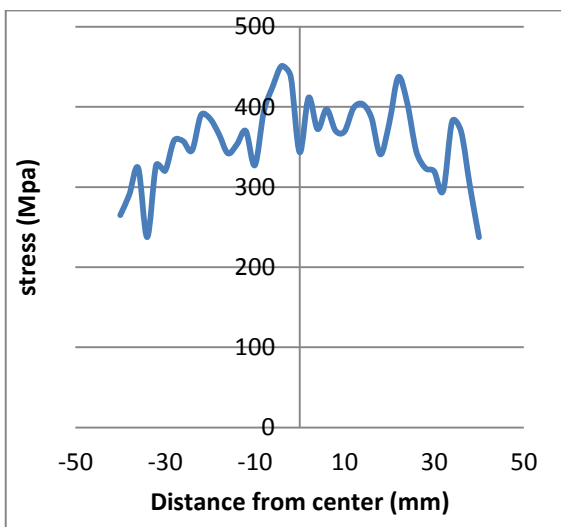
Figure 4.13 Crack formed during outside -in contour



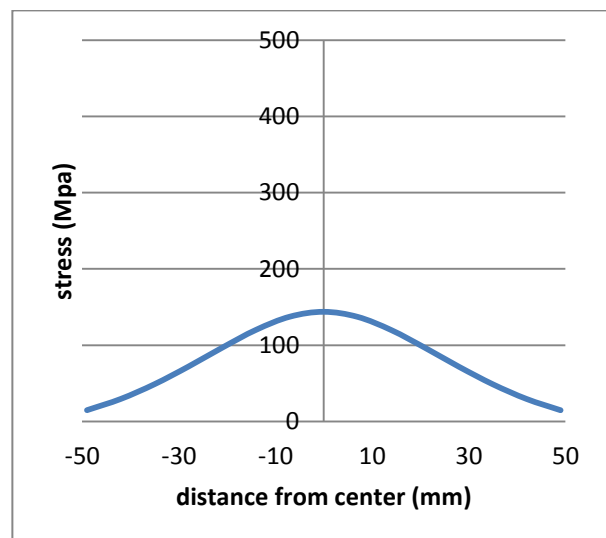
a) Experimental result along diagonal 1



b) Simulation result along diagonal 1

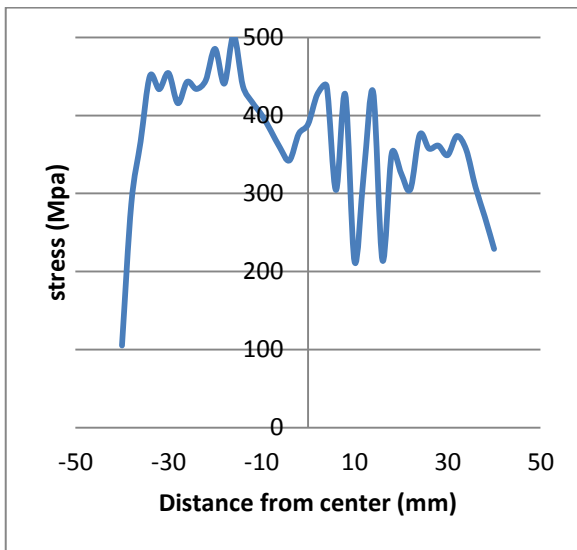


a) Experimental result along diagonal 2

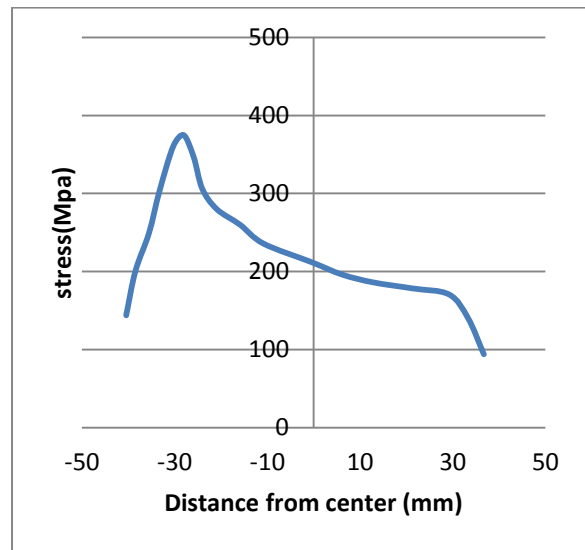


b) Simulation result along diagonal 2

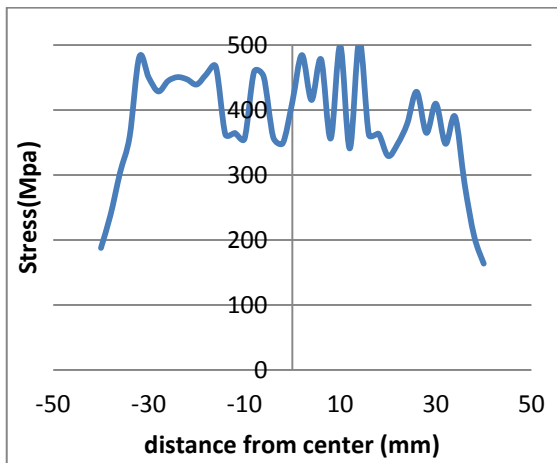
Fig 4.14 stress distribution on Inside-out contour area filling path



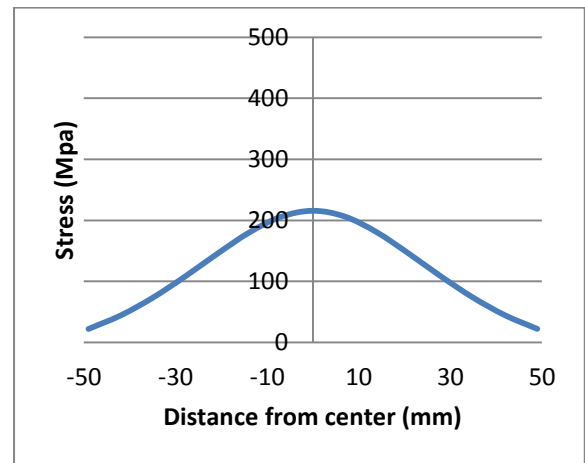
a) Experimental results along diagonal 1



b) Simulation result along diagonal 1



a) Experimental result along diagonal 2



b) Simulation result along diagonal 2

Fig 4.15 stress distribution in Zigzag area filling path

- The step over increment chosen for weld deposition process is 3mm. Here the heat energy distribution along the 3mm width varies along the center as shown in fig 3.1. But in simulation uniform heat flux is provided for the entire weld width.

The difference in residual stress values obtained during experimental and numerical may be because of the following reasons:

- In this finite element model only a moving heat source is considered while in the actual case the material deposition occurs which retains much more energy on the base plate.
- The base plates may be having built in residual stress that is being induced during the production since it undergoes melting and solidification in stages.

4.5 Summary

The results obtained from the Finite element analysis are verified experimentally and the stress distribution shows a remarkable resemblance to the experimental stress pattern. It may be noted that the residual stresses are influenced not by the temperature perse, but the difference in the temperature. Higher stresses are observed where the temperature gradients are steeper. Or in other words, if the heat input is distributed and is not concentrated at a point, residual stresses will be minimal. On the other hand, concentrated heat input, like the outside-in contour area filling path will lead to high residual stresses (and even possible cracks).

Chapter 5

Conclusion and Future Scope

5.1 Conclusion

In this work, a 3D finite element model was developed for weld-deposition AM process for different area filling path operations such as zig zag area filling path pattern, outside in contour area filling path pattern and Inside out contour area filling path pattern. The analysis is capable of predicting the temperature gradient and thermally induced stress distribution on the base plate due to the material deposition process. Finite element analysis is done using Ansys Mechanical APDL and it is validated experimentally. Experimental validation is done using AM system made by attaching GMAW system to a CNC machine and the residual stress is measured using XRD residual stress measuring instrument.

From the numerical and experimental results it is observed that, the temperature and residual stress are found to be high at the end point of the deposition path then it gradually reduces towards the edge. The numerical results show marginal deviation in values with comparison to the experimental value. This might be because of the reason that Material deposition is not considered in numerical method in experimental process, material deposition is considered. The stress values are obtained for the three area filling patterns, among those outside in contour shows the maximum stress concentration. In the experimental result obtained for outside in contour, it's found that the stress at the center i.e. the last point of the weld path is found to be dropping, this because of the crack formed at that point since the stress formed at that point is higher than the unlimited stress of that material.

After examining the weld deposition area numerically and experimentally the following conclusions can be made:

1. The developed Finite element modeling model for the weld deposition can be used as a viable option to understand the residual stress pattern.

2. The residual stress induced on weld plate is highly influenced by the path of area filling. It is found that even if the total heat induced to the base plate is same, the total residual stress on the plate varies. This occurs because of the accumulation of heat energy depending on the path followed which causes non uniform cooling.

5.2 Future Scope

Additive manufacturing of metals is in its incubation period, especially the research in the field of thermally induced residual stresses in metallic AM. The major challenge in the same was the absence of a dedicated finite element package for the analysis purpose. The APDL has tied Here an attempt is made to develop APDL code for the weld-deposition processes. There are number of limitations in the developed model. Here only moving heat source is considered while this can be further developed by material deposition so that the total residual stress of fully furnished model can be studied.

Here Residual stress is studied for models made by three different areas filling path patterns and found the best one that suits the purpose. The studies can be further progressed by studying the effect of relating the two or more patterns in a single layer or in multi-layer thereby managing the distribution of the thermally induced residual stress further.

Reference

- [1] I. Gibson, D. W. Rosen, and B. Stucker, *Additive manufacturing technologies*. Springer Science Business Media, 1007.
- [2] D. I. Wimpenny, B. Bryden, and I. R. Pashby, "Rapid laminated tooling," *J. Mater. Process. Technol.*, vol. 138, no. 1–3, pp. 214–218, Jul. 2003.
- [3] J.-P. Kruth, P. Mercelis, J. V. Vaerenbergh, L. Froyen, and M. Rombouts, "Binding mechanisms in selective laser sintering and selective laser melting," *Rapid Prototyp. J.*, vol. 11, no. 1, pp. 26–36, Feb. 2005.
- [4] T. J. Gornet, K. . Davis, T. . Starr, and K. . Mulloy, "Proceedings of the solid freeform fabrication symposium characterization of selective laser sintering materials to determine process stability," *Univ. Tex. Austin Usa*, 2002.
- [5] K. P. Karunakaran, S. Suryakumar, V. Pushpa, and S. Akula, "Retrofitment of a CNC machine for hybrid layered manufacturing," *Int. J. Adv. Manuf. Technol.*, vol. 45, no. 7–8, pp. 690–703, Dec. 2009.
- [6] M. Held, "ZigPocket: On the Computational Geometry of Zigzag Pocket Machining," in *CG International '90*, T.-S. Chua and T. L. Kunii, Eds. Springer Japan, 1990, pp. 281–296.
- [7] M. Held, "Voronoi diagrams and offset curves of curvilinear polygons," *Comput.-Aided Des.*, vol. 30, no. 4, pp. 287–300, Apr. 1998.
- [8] D. Rosenthal, "mathematical theory of heat distribution during welding and cutting," *Weld. J.*, vol. 20, no. 5, p. 220s–240s, 1941.
- [9] N. N. Rykalin, "Berechnung der Wärmevorgänge beim Schweißen", VEB Verlag Technik, Berlin, 1957(Original: "Raschety teplovykh protsessov pri svrake", Moscow, Mashgiz, 1951)
- [10] B. . Boley and J. . Weiner, "Theory of thermal stresses," *Dover Publ. Inc 1997 Org Publ John Wiley Sons Inc New York*, pp. 41–44, 1960.
- [11] J. Goldak and M. Bibbly, "Computational thermal analysis of welds: current status and future directions.," *Model. Cast. Weld. Process Iv*.
- [12] F. Kong and R. Kovacevic, "3D finite element modeling of the thermally induced residual stress in the hybrid laser/arc welding of lap joint," *J. Mater. Process. Technol.*, vol. 210, no. 6–7, pp. 941–950, Apr. 2010.
- [13] F. Kong, J. Ma, and R. Kovacevic, "Numerical and experimental study of thermally induced residual stress in the hybrid laser–GMA welding process," *J. Mater. Process. Technol.*, vol. 211, no. 6, pp. 1102–1111, Jun. 2011.

- [14] D. Deng and S. Kiyoshima, "Numerical simulation of welding temperature field, residual stress and deformation induced by electro slag welding," *Comput. Mater. Sci.*, vol. 62, pp. 23–34, Sep. 2012.
- [15] D. Stamenković and I. Vasović, "finite element analysis of residual stress in butt welding two similar plates," *Sci. Tech. Rev.*, vol. LIX, no. 1, pp. 57–60, 2009.
- [16] Hani Aziz Ameen, Khairia Salman Hassan, and Muwafaq Medi Salah, "Influence of the butt joint design of TIG welding on the thermal stresses," *Eng. Tech. J.*, vol. 29, no. 14, pp. 2841–2849, 2011.
- [17] P. . Sudershenan and U. . Kempiah, "The effect of heat input and travel speed on the welding residual stress by finite element method," *Int. J. Mech. Prod. Eng. Res. Dev. Ijimperd*, vol. 2, no. 4, pp. 43–50, Dec. 2012.
- [18] I. R. Nodeh, S. Serajzadeh, and A. H. Kokabi, "Simulation of welding residual stresses in resistance spot welding, FE modeling and X-ray verification," *J. Mater. Process. Technol.*, vol. 205, no. 1–3, pp. 60–69, Aug. 2008.
- [19] A. Yaghi, T. H. Hyde, A. A. Becker, W. Sun, and J. A. Williams, "Residual stress simulation in thin and thick-walled stainless steel pipe welds including pipe diameter effects," *Int. J. Press. Vessels Pip.*, vol. 83, no. 11–12, pp. 864–874, Nov. 2006.
- [20] s subramaniam, D. R. White, J. E. jones, and D. W. Lyons, "Experimental approach to selection of pulsing parameters in pulsed GMAW," *Am. Weld. Soc.*, pp. 166–172, Jun. 1999.
- [21] amudala babu and lakshmana kishore, "Finite element simulation of hybrid welding process for welding 304 austentic stainless steel plate," *ijret*, vol. 1, no. 3, pp. 401–410, Nov. 2012.
- [22] F. Prinz and C. M. U. E. D. R. Center, "Processing, thermal, and mechanical issues in shape deposition manufacturing," *Dep. Electr. Comput. Eng.*, Jan. 1995.
- [23] N. . Klingbeil, J. . Beuth, R. . Chin, and C. . Amon, "Residual stress-induced warping in direct metal solid freeform fabrication," *Int. J. Mech. Sci.*, vol. 44, no. 1, pp. 57–77, Jan. 2002.
- [24] V. Pavelic, R. Tanbakuchi, O. A. Uyehara, and Myers, "Experimental and computed temperature histories in tungsten arc welding of tin plates," *Welding J. Res. Suppl.*, vol. 48, p. 295s–305s, 1969.
- [25] J. Goldak, A. Chakravarti, and M. Bibby, "A new finite element model for welding heat sources," *Met. Trans. B*, vol. 15, no. 2, pp. 299–305, Jun. 1984.
- [26] Ansys 13 manual